

Curriculum Vitae

Allen Abey Alexander

Educational Background

- Masters' (M.S) candidate

Major: Cellular and Molecular Biomedical Sciences (2015-2017) University of Maryland, Baltimore; Maryland, USA

- Bachelors' (B.Tech)

Major: Biotechnology (2011-2015), Vellore Institute of Technology, Tamil Nadu, India

Publication

Published Articles

- Javed Mahmood, Sarthak R. Zaveri, Stephanie C. Murti, **Allen Alexander**, Caroline Connors, Hem D. Shukla, Zeljko Vujaskovic: *Caveolin-1: A novel prognostic biomarker of radioresistance in cancer.*. International Journal of Radiation Biology 08/2016; <http://dx.doi.org/10.1080/09553002.2016.1222096>
- K. Lohitesh, A.K. Behera, **A.A. Alexander**, V. Suneetha: Detection and removal of hydrogen sulphide gas from food sewage water collected from vellore. Der Pharmacia Lettre 01/2013; 5(3). <http://scholarsresearchlibrary.com/dpl-vol5-iss3/DPL-2013-5-3-163-169.pdf>

Poster Publication

- **Allen A. Alexander**, Caroline Q. Connors, Sarthak Zaveri. Stephanie Murti, Hem Shukla, Javed Mahmood* and Zeljko Vujaskovic; Caveolin-1: A Novel Prognostic Biomarker for Radioresistance in Non-Small Cell Lung Carcinoma (NSCLC) and

Prostate Cancer, American Society of Therapeutic Radiology and Oncology (2016), Boston, Massachusetts.

- Caroline Q. Connors, **Allen A. Alexander**, Radmila Pavlovic,, Javed Mahmood*, Daniel Weinrich, Hotaka Matsui, John Eley, Isabel L Jackson, and Zeljko Vujaskovic; Elucidation of the molecular mechanism of Radiation-induced Erectile Dysfunction, American Society of Therapeutic Radiology and Oncology (2016), Boston, Massachusetts.

Funded Grants

- Department of Translational Radiation Sciences (DTRS) Departmental Seed Research Grant; Principal Investigator: Javed Mahmood.
- Pancreatic Cancer Research Departmental Seed Grant; Principal Investigator: Javed Mahmood.
- Cancer Research Funds by Hilgenberg Family Foundation Grant; Principal Investigator: Javed Mahmood.

Awards

- Jindal South West Academic Excellence Award (2012-2014)
- Jindal South West Foundation Student Scholarship (2011-2014)

Abstract

Title of Dissertation: Tripartite treatment by radiation, hyperthermia and anti-OX40 immunotherapy potentiates tumor growth delay and tumor microenvironment immunomodulation in pancreatic cancer.

Allen Abey Alexander, Master of Science, 2017

Dissertation Directed by: Javed Mahmood, PhD, Assistant Professor, Department of Translational Radiation Sciences (DTRS).

Pancreatic cancer is the fourth most deadly cancer in the United States. Despite development in conventional treatment strategies the 5 year survival rate is only 7.7%. In this study we demonstrated that the tripartite treatment by combination of fractionated radiation therapy, hyperthermia and anti-OX40 immunotherapy (tripartite) led to significant impact on pancreatic cancer in mice. The treatment of mice with the tripartite treatment demonstrated significant tumor growth inhibition ($p < 0.0001$) with no observable toxicity due to this treatment. Flow cytometric analysis of the tumor showed a shift in tumor microenvironment from immune suppressive to immune stimulatory with significantly higher CD4+ and CD8a+ ($p < 0.05$) T lymphocytes. A significantly higher population of helper T cells and cytotoxic T cells was observed in the usually immune-deficient pancreatic cancer tumor microenvironment coupled with a decrease in the immunosuppressive microenvironment in the tumors of animals receiving the tripartite treatment is potentially the cause of the superior anti-tumor effect observed in animals receiving the tripartite treatment.

Tripartite Treatment by Radiation, Hyperthermia and Anti-OX40 Immunotherapy Potentiates
Tumor Growth Delay and Tumor Microenvironment Immunomodulation in Pancreatic
Cancer

by
Allen Abey Alexander

Thesis submitted to the Faculty of the Graduate School of the
University of Maryland, Baltimore in partial fulfillment
of the requirements for the degree of
Master of Science
2017

Acknowledgements

I would like to express my heartfelt gratitude to my mentor Dr. Javed Mahmood for allowing me to work on this project and his continued support.

I would like to thank my thesis committee members Dr. Eduardo Davila and Dr. Juong G. Rhee for their constant support and guidance throughout the study.

I also would like to extend my thanks to my lab mates Caroline Connors, Sandrine Soman and Santanu Samanta.

In addition I would like to thank Dr. Xiaoxuan Fan, Karen Underwood, Lorenzo Stramucci, Dr. France Carrier, Dr. Zeljko Vujaskovic, Dr. Regine Williams and John Hilgenberg for their constant support and assistance in different arms of the study.

Finally I would like to be grateful for my parents for their unwavering belief and loving support for me.

Table of Contents

Chapter	Page number
Curriculum Vitae	
Abstract	
Title Page	
Acknowledgement	iii
List of Figures	viii
List of Abbreviations	x
1. Understanding Pancreatic Cancer	1
1.1. Introduction.....	1
1.2. Pancreatic cancer statistics.....	3
1.3. Pancreatic Cancer Treatment	3
1.4. Hurdles in Pancreatic Cancer Treatment.....	5
1.5. Pancreatic cancer and immune microenvironment.....	6
1.6. Pancreatic Cancer and Radiation Therapy.....	9
1.7. Pancreatic Cancer and Hyperthermia.....	10
2. Proposed Experimental Hypothesis.....	12
2.1. Experimental Groups.....	13
2.2. Flow Cytometry Markers.....	13
3. Experimental Design	14
3.1. Printing 3D accessories for Experiment.....	14

3.1.1. Print design for 3D accessories.....	14
3.2. Methods.....	16
3.2.1. Syngeneic Subcutaneous Tumor Model Development.....	16
3.2.1.1. Cell Culture.....	16
3.2.1.2. Anesthetizing pre injection.....	16
3.2.1.3. Subcutaneous injection.....	17
3.2.2. Tumor Volume Measurement.....	17
3.2.3. Animal Monitoring.....	18
3.2.3.1. Body Weight Measurements.....	18
3.2.3.2. Transporting of Animals	19
3.2.3.3. Evaluation of rodent incisors.....	19
3.2.4. Hyperthermia Protocol.....	21
3.2.4.1. Anesthesia.....	21
3.2.4.2. Hyperthermia Water Bath.....	23
3.2.4.3. Hyperthermia Treatment Dosage.....	24
3.2.5. Radiation Protocol.....	25
3.2.5.1. Anesthesia.....	26
3.2.5.2. Pancreatic Tumor Imaging.....	26
3.2.5.3. Non-invasive imaging procedure (CT).....	26
3.2.5.4. Animal CT Imaging.....	27
3.2.5.5. Tumor Irradiation.....	27
3.2.5.6. Supportive care.....	28
3.2.6. Immunotherapeutic Treatment.....	28

3.2.6.1.	Drug Preparation.....	29
3.2.6.2.	Intraperitoneal (I.P) injection.....	30
3.2.7.	Euthanasia Criteria and Graphical depiction.....	30
3.2.8.	Flow Cytometry.....	31
3.2.8.1.	Organ Processing.....	31
3.2.8.1.1.	Processing tumor.....	31
3.2.8.1.2.	Processing blood.....	31
3.2.8.2.	Staining Protocol.....	32
3.2.8.3.	Fixing Sample after Staining	32
3.2.8.4.	Flow cytometry Analysis.....	32
3.2.9.	Statistical Analysis.....	33
4.	Results.....	34
4.1.	Tumor Regression Study.....	34
4.1.1.	Tumor Survival.....	34
4.1.2.	Body Weight.....	34
4.1.3.	Tumor Volume Regression.....	35
4.2.	Immunological Analysis.....	38
4.2.1.	Flow cytometry.....	38
5.	Discussion.....	42
5.1.	Tumor Growth Delay.....	42
5.2.	Flow Cytometric Analysis.....	45
6.	Conclusion.....	48
7.	Future Directions and Potential Caveats.....	49

8.	Supplementary Figures.....	51
9.	References.....	53

List of Figures

Figure	Title	Page Number
1	Schematic for pancreatic cancer statistics	1
2	Pancreatic Cancer Microenvironment.....	4
3	Schematic for pancreatic cancer treatment strategies.....	5
4	Histopathological depiction for human pancreatic cancer.....	7
5	Hyperthermia administration platform.....	14
6	Isoflurane administration platform.....	15
7	Mouse origin pancreatic cancer (Panc02) cell line culture.....	16
8	Rodent incisor evaluation depiction.....	21
9	Hyperthermia administration water bath setup.....	23
10	Kaplan Meier survival Plot.....	34
11	Body weight plot.....	34
12	Normalized tumor volume plot among all study groups.....	35
13	Normalized tumor volume plot among treatment groups.....	36
14	Final tumor volume plot among all study groups.....	36
15	Histogram comparing final tumor volume between all study groups.....	37

16	Histogram comparing final tumor volume between treatment groups.....	37
17	Flow cytometric outcome for T cell expression in tumors at 10 day.....	38
18	Flow cytometric outcome for T cell expression in tumors at 45 day.....	39
19	Histogram depicting the expression of PD-1 and LAG3 at 10 and 45 days.....	40
20	Histogram depicting MDSCs marker expressing population at 10 and 45 days.....	41
Supplementary		
Figure 1	Tumor weight aligned dot plot.....	51
Supplementary		
Figure 2	Histogram depiction of flow cytometric analysis outcome of blood at 10 days.....	52

List of Abbreviations

PDAC – Pancreatic ductal adenocarcinoma

EGFR – Epidermal growth factor receptor

FOLFIRINOX –Folinic acid, 5-fluorouracil, irinotecan, and Oxaliplatin

ECM – Extracellular Matrix

IDO - Indoleamine 2, 3-dioxygenase

Tregs - T regulatory cells

PD-1 – Programmed death receptor -1

PD-L1 – Programmed death receptor ligand -1

DCs – Dendritic cells

MHC – Major Histocompatibility Complex

LAG3 – Leukocyte activating gene 3

MDSCs – Myeloid Derived suppressor cells

CD – Cluster of Differentiation

NK – Natural Killer

HSPs - Heat Shock Proteins

PSA – Prostate Specific Antigen

STL – STereo-Lithography

PLA - Poly Lactic acid

PVA – Poly Vinyl Alcohol

EDTA – Ethylene Diamine Tetra-acetic acid

DMSO – Dimethyl Sulfoxide

PBI – Partial Body Irradiation

3D – 3 Dimensional

VR – Veterinary Resources

SARRP - Small Animal Radiation Research Platform

CT – Computer Tomography

IACUC - Institutional Animal Care and Use Committee

IP - Intraperitoneal

PBS – Phosphate Buffer Saline

RBC – Red Blood Cells

FBS – Fetal Bovine Saline

FACS – Fluorescence Activated Cell Sorting

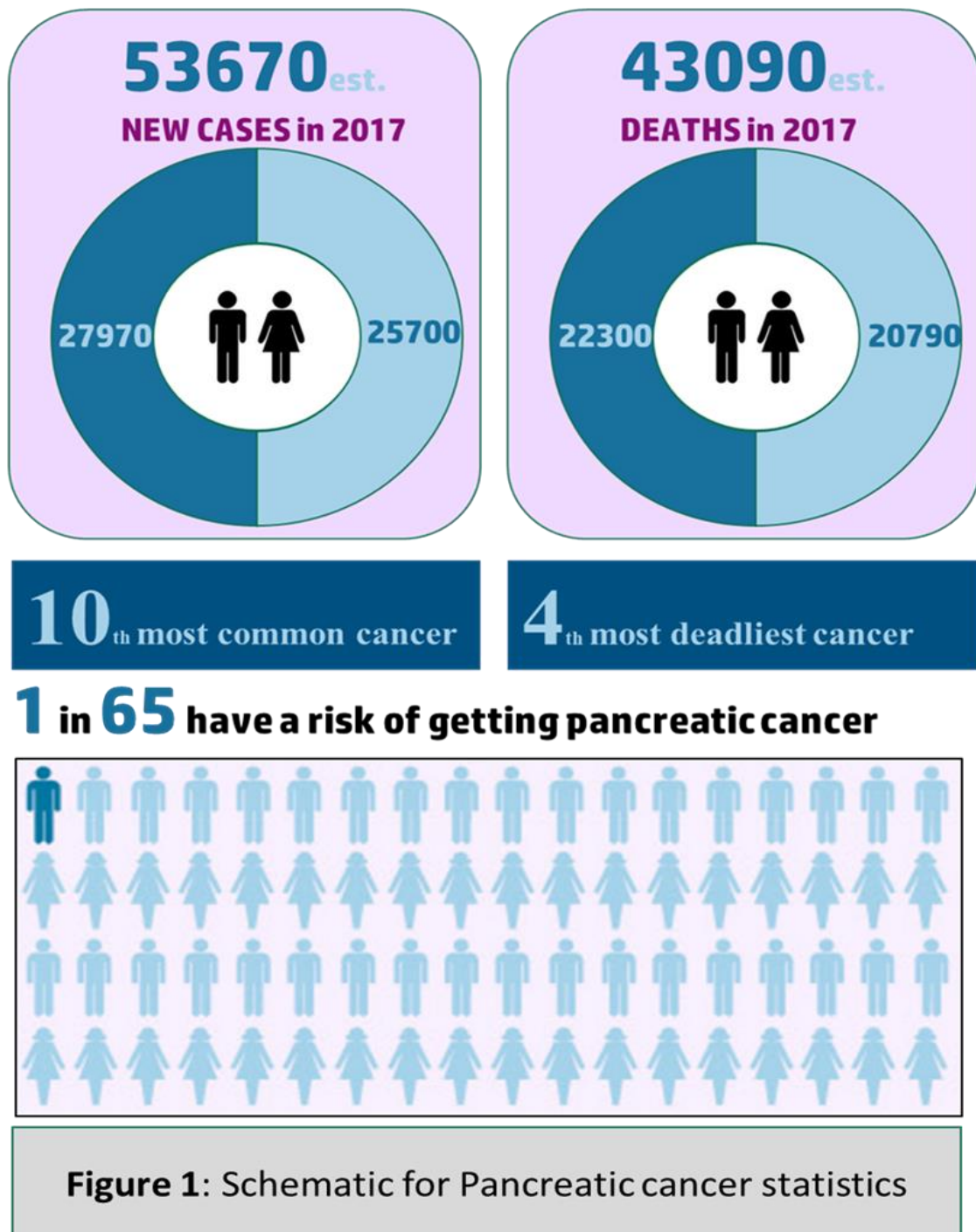
SEM – Standard Error of Mean

ANOVA – Analysis of Variance

Chapter 1: Understanding Pancreatic Cancer

1.1. Introduction

Cancer is a major public health problem worldwide and is the second-leading cause of death in the United States. A total of 1,688,780 cases of cancer is estimated to be



diagnosed in 2017. Among this pancreatic cancer is the fourth most deadly cancer in the United States with an estimated 53,670 diagnosis and out of which a predicted 43,090 deaths in the year 2017 (Figure 1) (Siegel, Miller and Jemal, 2017). Pancreatic cancer is characterized as a disease in which normal healthy pancreas cells lose their normal functionality and grow uncontrollably to form tumors. The tumor may turn cancerous and metastasize to different parts of the body through the blood vessels. Based on the where cancer began, the tumors may be exocrine and endocrine in origin and therefore classified accordingly (Melorose *et al.*, 2008; Zheng *et al.*, 2014; Singh *et al.*, 2015).

According to the Pancreatic Cancer Action Network estimates deaths associated with pancreatic cancer will be second to only lung cancer by 2020. Surgery and chemo-radiation therapy are the primary treatment strategies for pancreatic cancer in patients. However, despite all the current treatment available, the one-year survival rate of patients with pancreatic cancer is only 20% and five-year survival of a meager 7.7% (Li *et al.*, 2004; Vincent *et al.*, 2011; Patrick Michl, 2013).

Pancreatic cancer affects men more than women by a factor of 1.1 approximately. This difference though not very significant is a crucial factor to consider while designing study. Pancreatic cancer accounts for 3% of all diagnosed cancers and 7% of all cancer deaths in the United States. The average lifetime risk of pancreatic cancer for both men and women is about 1 in 65 (1.5%) (Guidelines, 2005; Siegel, Miller and Jemal, 2017).

1.2.Pancreatic Cancer Treatment Statistics

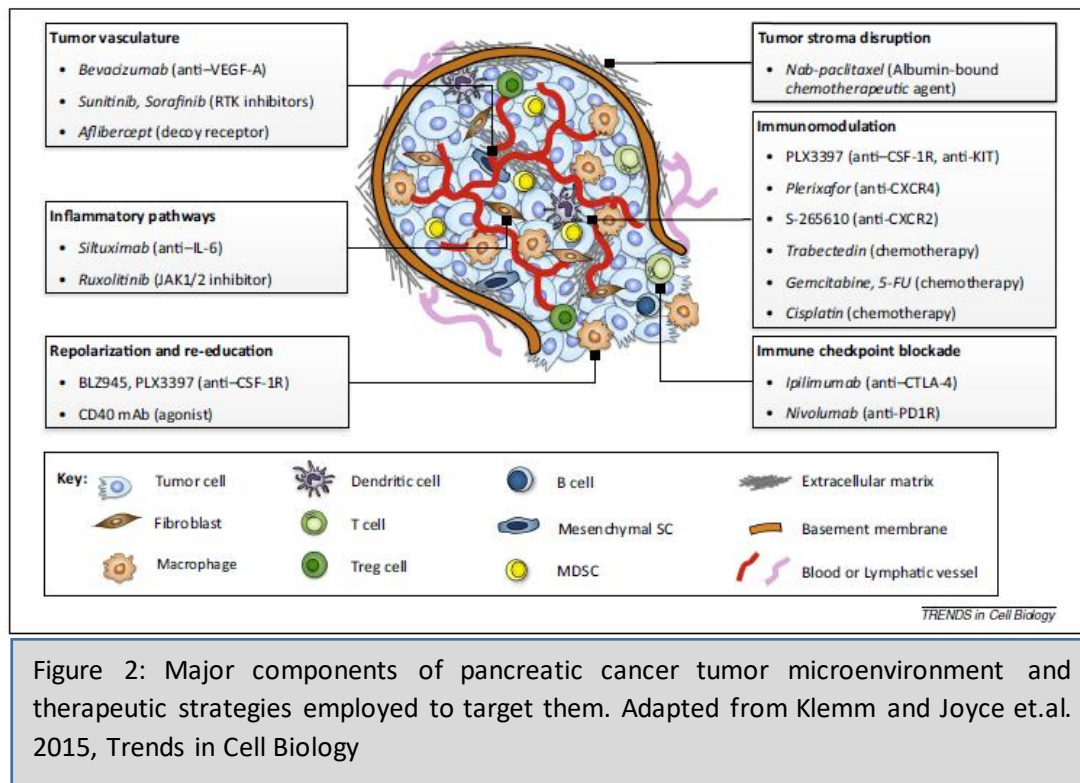
Pancreatic cancer is particularly difficult to diagnose during early stages of cancer development compared to other cancer. An estimated 52% of patients having the distant disease and 26% showing localized spread. Pancreatic Ductal Adenocarcinoma (PDAC) accounts for 80% of the total pancreatic cancer diagnosis, out of which as low as 2% of these exocrine tumors are benign. PDAC in itself is a highly lethal malignancy because of approximately 80% of patients present with locally advanced diseases. In these patients, the use of surgery is not recommended and therefore is a significant population in immediate need for alternative effective medical interventions.

This cancer is also largely resistant to chemotherapy and radiation therapy, leading to five-year survival statistic of less than 6%. In response, multiple strategies targeting the tumor cellular elements of desmoplasia to alleviate intratumoral pressure and local immune modulation have been investigated but remain to be accepted as reliable alternate treatment strategies (Guidelines, 2005; Stathis and Moore, 2010; Garrido-Laguna and Hidalgo, 2015).

1.3.Pancreatic Cancer Treatment

Standard treatment for pancreatic cancer is a combination of surgery, radiation therapy, and chemotherapy. For the treatment of resectable and borderline resectable tumors, surgery is the prefer mode of therapy. If the tumor has invaded beyond the pancreas, then chemotherapy or radiation therapy may be administered to reduce the size to a

resectable volume followed by surgery. However despite all the current advancements in cancer therapies the 5-year survival of a very low 7.7%. Consequently, novel treatment strategies for pancreatic cancer treatment are desperately needed (Figure 3). (Froger, 2003; Demaria *et al.*, 2004, 2005; Li *et al.*, 2004; Guidelines, 2005; Stathis and Moore, 2010; Feig *et al.*, 2012; Valsecchi *et al.*, 2014)



However, the lack of early diagnosis strategies and screening biomarkers is a major constraint in the treatment of pancreatic cancer. Therefore, the majority of patients are diagnosed with advanced and metastatic diseases. Therefore only 10-15% of these patients are eligible for surgical resection. However, even after surgery, a majority of the candidates relapse even when coupled with adjuvant systemic therapies.

In respect to chemotherapy, a standard of care for pancreatic cancer in patients is Gemcitabine. However, it demonstrates only modest improvement in the survival of patients. Several targeted therapies like therapies by Erlotinib inhibiting epidermal growth factor receptor (EGFR) tyrosine kinase when combined with Gemcitabine increased the overall survival by 0.33 months. Combination chemotherapy FOLFIRINOX (oxaliplatin, irinotecan, leucovorin and 5-fluorouracil) evaluated in the PRODIGE project demonstrated improved the survival of patients with metastatic pancreatic cancer by 4.3 months. (Ma and Hidalgo, 2013)(Li *et al.*, 2004; Vazquez *et al.*, 2008; Hirschhorn-Cymerman *et al.*, 2009; Vincent *et al.*, 2011; Safe, 2015; Singh *et al.*, 2015) (Figure 3)

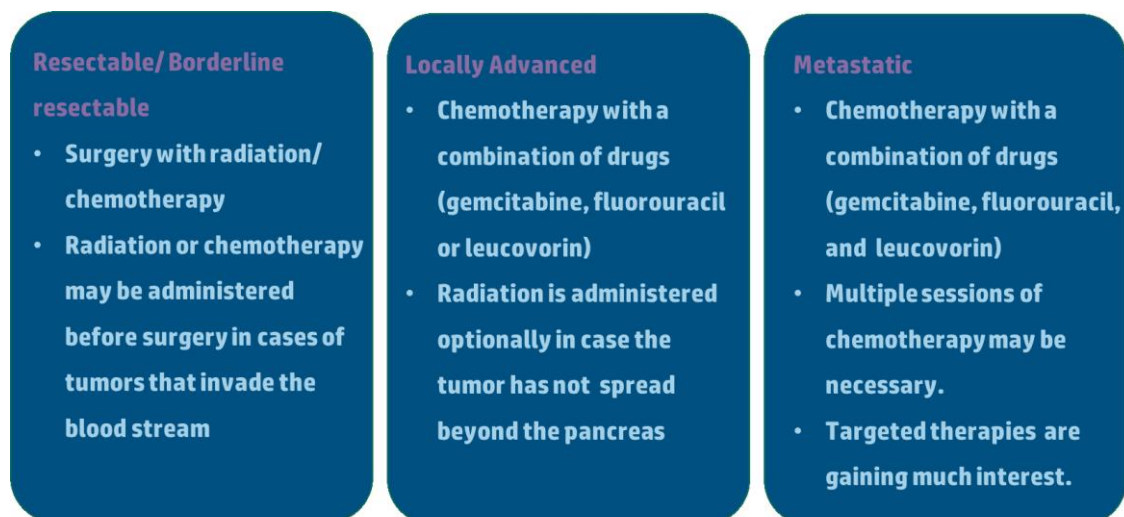


Figure 3: Schematic for Pancreatic Cancer treatment strategies

1.4.Hurdles in Pancreatic Cancer Treatment

The tumor microenvironment is a major problem associated with the translatability of pancreatic cancer treatment, accounting for the lack of success in the treatment of

patients despite the success in vitro and in vivo small animal studies. PDAC is a stroma rich cancer, which significantly outnumbers the cancer cells. The tumor stroma is rich in fibroblasts, myofibroblasts, immunological cells, stellate cells, extra-cellular matrix (ECM), cytokines and growth factors. In pancreatic cancer a massive influx of immunosuppressive leukocytes into the tumor microenvironment (Fresno Vara *et al.*, 2004; Ikemoto *et al.*, 2006; Vasievich and Huang, 2011; Coussens, Zitvogel and Palucka, 2013; Klemm and Joyce, 2015) (Figure 2).

1.5. Pancreatic Cancer and Immune Microenvironment

a) Overview

Pancreatic cancer is a classified stroma rich tumor (Figure 4). However, this induces local and systemic dysfunction or immunosuppression. Pancreatic cancer interferes with antigen cross-presentation for effector T cells by downregulating MHC class I complex. In pancreatic cancer tumors, IDO (Indoleamine 2, 3-dioxygenase) suppresses T-lymphocytes by starving them and thereby leading to the development of tumor-derived antigen tolerance. IDO also results in increased expression of Tregs (T regulatory cells) in the lymph nodes of metastatic pancreatic cancer tumors. In pancreatic cancer, PD-L1 is also expressed that suppresses the activity of effector cells (Ikemoto *et al.*, 2006; Nomi *et al.*, 2007; Vasievich and Huang, 2011; Sideras *et al.*, 2014; Postow, Callahan and Wolchok, 2015).

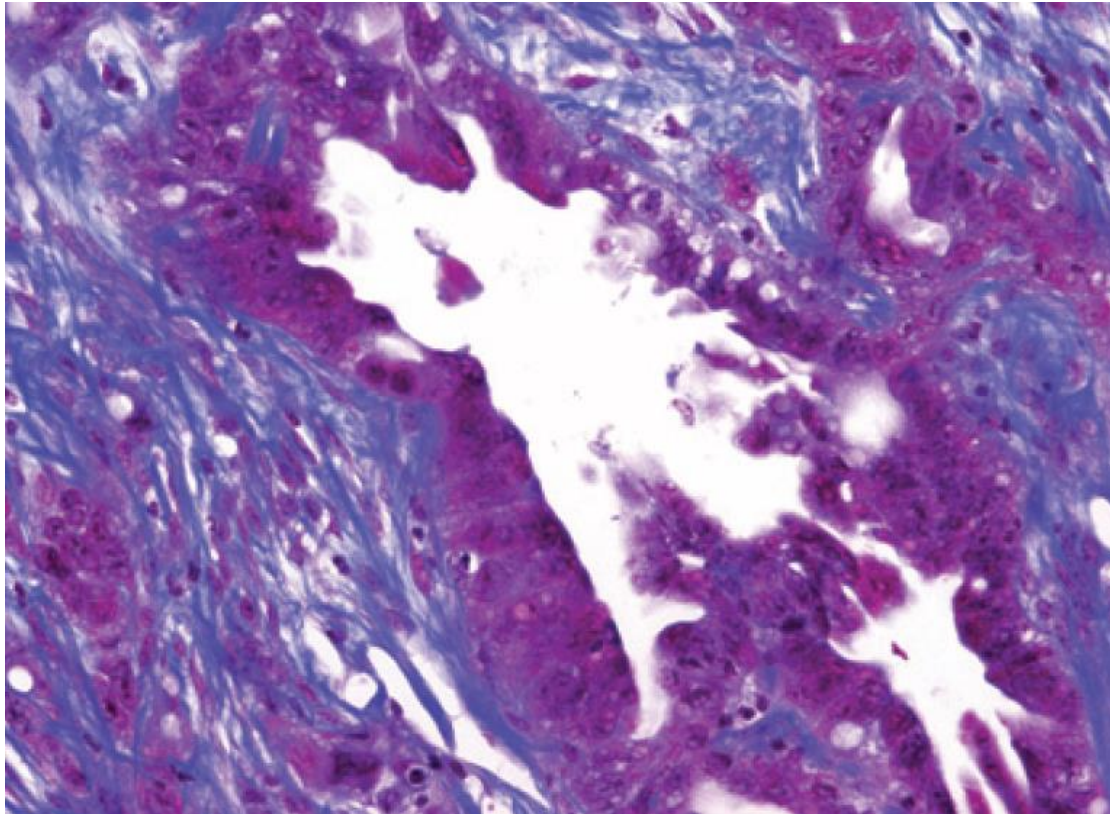


Figure 4: Representative of stroma rich pancreatic cancer tumor microenvironment shown by Masson's trichrome assay. Adapted from Feig et.al. 2012, Clinical Cancer Research

b) Role of regulatory and helper T lymphocytes

CD4⁺ T cell population activate innate immune cells such as macrophages, B-lymphocytes, and CD8⁺ effector T-lymphocytes through cytokine secretion and direct cell to cell signaling. CD4⁺ T lymphocytes population decreased in the pancreatic cancer patients compared to healthy patients. The number of the CD4⁺ T cells was reportedly lower in pancreatic cancer than chronic pancreatitis. The proliferation and migration of CD4⁺ T cells are significantly inhibited in pancreatic cancer microenvironment. This is a crucial factor in the survival of pancreatic cancer patients favoring higher survival rate. (Field *et al.*, 2003; Nascimbeni *et al.*, 2004; Parel and Chizzolini, 2004; Ikemoto *et al.*, 2006; Ahmadzadeh *et al.*, 2009; De Monte *et al.*, 2011; Gu *et al.*, 2012).

c) Role of cytotoxic and effector T lymphocytes

Also, CD8⁺ T-cells are deactivated in pancreatic cancer patients, contributing to the advancement of tumor stage and reduction in survival of patients. Similar outcomes are also associated with natural killer (NK) cells deactivation in tumor microenvironment further impeding tumor survival in patients. In pancreatic cancer microenvironment antigen presentation is significantly downregulated promoting increase survival in these patients. The presence of mast cells in the pancreatic cancer microenvironment increase the metastasis rate in the patients. The expression of OX-40 an essential receptor complex that is correlated with better survival and is found in high concentration in activated T cells (Hirschhorn-Cymerman *et al.*, 2009; Gough *et al.*, 2010; Gu *et al.*, 2012; Curti *et al.*, 2013).

d) Dendritic cells

Dendritic cells (DCs) is uncommon in pancreatic cancer microenvironment and the circulating blood, however having higher circulating DCs count is associated prolonged survival in patients. LAG3 marker is a major indicator for the development of dendritic cells to mature DCs. The primary role of mature DCs is activation of CD4⁺ and CD8⁺ T cells through capture, internalization, processing and presentation of antigen by the MHC class I and II molecules. In pancreatic cancer tumors, the DCs occupy mainly the edges of the tumor and lead to impairment of DCs functionality. The addition to the maturation of DCs function LAG3 cell marker demonstrates immune-suppressive activity in the tumor microenvironment. (Field *et al.*, 2003; Nascimbeni *et al.*, 2004; Laheru and Jaffee, 2005; Ahmadzadeh *et al.*, 2009; Vincent *et al.*, 2011; Moran, Kovacsovics-Bankowski and Weinberg, 2013; Victor *et al.*, 2015).

e) Programmed Death receptor expressing cells

Similarly, the PD-1 receptor is a significant marker for activated and exhausted T lymphocytes. There are conflicting beliefs about the functionality of PD-1 receptor activity. PD-1 demonstrates both immune-stimulating and immune-suppressive activity in the tumor microenvironment of pancreatic tumor of patients. Therefore the employment of PD-1 and PDL-1 targeting treatments having been gaining much interest in recent times (Field *et al.*, 2003; Nascimbeni *et al.*, 2004; Parel and Chizzolini, 2004).

f) Myeloid-derived suppressor cells

Myeloid-derived suppressor cells (MDSCs) are a mixture of immature myeloid cells including immature stages of macrophages, granulocytes, and DCs. MDSCs comprise two types of cells, polymorphonuclear granulocytic MDSCs, and mononuclear monocytic MDSCs. MDSCs are usually associated with an immune suppressive tumor microenvironment in both animals and humans. In mice, CD11b and Gr-1 are characteristic of MDSCs and lack the markers of mature myeloid cells. (Field *et al.*, 2003; Nascimbeni *et al.*, 2004; Laheru and Jaffee, 2005; Ahmadzadeh *et al.*, 2009; Vincent *et al.*, 2011; Moran, Kovacsovic-Bankowski and Weinberg, 2013; Victor *et al.*, 2015).

1.6. Pancreatic Cancer and Radiation Therapy

Pancreatic cancer treatment with radiation therapy is in most cases is administered to reduce tumor to a negative margin (R0) gradient to facilitate surgical resection. Despite all the advances in the tumor treatment concepts and strategies, surgical resection is

currently the only means for tumor growth control and cure. Also, the clinical signs of pancreatic cancer are not usually detected in the advanced stages of pancreatic cancer. In earlier studies involving pancreatic cancer patients with non-resectable tumors are administered chemotherapy and radiation therapy to demonstrate clinical benefits (Formenti and Demaria, 2013; Moncharmont *et al.*, 2014; Morgan and Lawrence, 2015).

Regardless of the innovative development of the therapeutic strategies for radiation therapy strategies, the 5-year overall survival is minuscule. However, with these treatments only, 19-30% of the tumor become resectable. Tumor microenvironment of pancreatic cancer has a profound cytotoxic effect on the tumor cells due to radiation treatment. This tumor killing environment significantly impacts the therapeutic response, but the impact on the microenvironment signals several pathways due to the lack of oxygenation to the tumors leading to radioresistance. (Rotstein *et al.*, 1985; Ohuchida *et al.*, 2004; Melorose *et al.*, 2008; Chuong *et al.*, 2013; Hein, Ouellete and Yan, 2014; Sideras *et al.*, 2014; Safe, 2015; Victor *et al.*, 2015).

1.7.Pancreatic Cancer and Hyperthermia

Hyperthermia as an adjuvant therapy for radiation therapy and chemotherapy to increase the efficiency of these treatments. The combination of hyperthermia with immunotherapy is an attractive approach for the treatment of cancer, especially in stroma rich tumors like pancreatic cancer. Heat shock proteins (HSPs) like HSP70 and HSP90 are key players in the promotion of immune system. Hyperthermia involving

high temperatures induces cytotoxicity and causes direct killing of tumor cells. HSPs demonstrate contradictory results when investigating tumor killing activity. The involvement of HSPs indicates an involvement with the promotion of anti-apoptotic pathway. However, the immune system has adapted to employ HSPs as danger signals to induce an aggravated immune response (Malyutina *et al.*, 2005; Teng *et al.*, 2010).

HSPs released from these stressed or dying cells DCs to mature antigen presenting cells (APCs). Also by the endocytosis of HSPs by DCs increases the expression of Major Histocompatibility Complex (MHC) class II potentiating the immune recognition of antigens. Also, hyperthermia has been used effectively as a radiation sensitizer in locally advanced and recurrent solid tumors like in the case of breast, head and neck, and prostate tumors. The maturation step enables dendritic cells to cross-present tumor peptides that are released from local tumor hyperthermia treated tumor cells to class I-dependent CD8⁺ T cells. Various immunotherapeutic approaches are being evaluated in patients with metastatic prostate cancers by inducing systemic immunity to antigens such as PSA. Prostate cancer cells are inefficient in their antigen presenting capacity, as they frequently do not express molecules necessary for antigen processing and presentation. Also, they lack T-cell costimulatory molecules (CD80 and CD86) and, therefore, could potentially induce anergy of T cells. Thus, the major hurdle in inducing tumor-specific immunity against prostate cancer is the presence of inefficient antigen presentation by tumor cells (Malyutina *et al.*, 2005; Chatterjee, Diagaradjane and Krishnan, 2011; Gu *et al.*, 2012; Soares *et al.*, 2012).

Chapter 2: Proposed Experimental Hypothesis

Null Hypothesis: Combination therapy with fractionated radiation, hyperthermia and anti-OX40 immunotherapy does not demonstrate any significant difference in tumor growth inhibition and tumor microenvironment immune modulation.

Alternate Hypothesis: Combination therapy with fractionated radiation, hyperthermia and anti-OX40 immunotherapy shows a significant difference in tumor growth inhibition and tumor microenvironment immune modulation.

Specific Aim 1: Elucidate the effects of tripartite treatment by radiation, hyperthermia, and immunotherapy in pancreatic cancer.

- A. Demonstrate the effect of tripartite treatment in increased tumor regression in subcutaneous pancreatic cancer
- B. Evaluate if there are any toxic effects of the tripartite treatment in pancreatic cancer in mice.

Specific Aim 2: Elucidate the effects of the tripartite treatment on the immune systems.

- A. Evaluate the expression of helper and cytotoxic T-lymphocytes in the blood and tumor.
- B. Evaluate the expression of MDSC and OX40 expressing cells in the blood and tumor.

2.1. Experimental Groups

- | | |
|--------------------------------|--------------------------------|
| a) No treatment | f) Radiation with Anti-OX40 |
| b) Radiation | Immunotherapy |
| c) Hyperthermia | g) Hyperthermia with Anti-OX40 |
| d) Anti-OX40 Immunotherapy | Immunotherapy |
| e) Radiation with Hyperthermia | h) Tripartite Treatment |

2.2. Flow Cytometry Markers

Panel 1

- a) Anti-mouse CD4 – PE/Cy7 (Bio Legend, Catalog # 100421)
- b) Anti-mouse CD8a – FITC (Bio Legend, Catalog # 100705)
- c) Anti-mouse CD134 – APC (Bio Legend, Catalog # 119413)
- d) Anti-mouse PD-1 (CD279) – PE (Bio Legend, Catalog # 135205)
- e) Anti-mouse LAG-3(CD223) – Brilliant Violet 421(Bio Legend, Catalog # 125221)

Panel 2

- a) Anti-mouse Ly6G/Ly6C (Gr-1) – Alexa Fluor 647 (Bio Legend, Catalog # 108420)
- b) Anti-mouse CD11b – FITC (Bio Legend, Catalog # 101205)

Chapter 3: Experimental Design

3.1. Printing 3D accessories for Experiment

3.1.1. Print design for 3D Accessories

The experimental two-dimensional model was generated in a 3-dimensional design program (123D Design). The two-dimensional sketch is extruded to create the design to be printed. All the individual parts are grouped together, and all segment were verified for structural integrity and stability. The 3-dimensional model was exported in STL (STereoLithography) format, to be printed on a 3-D printer.

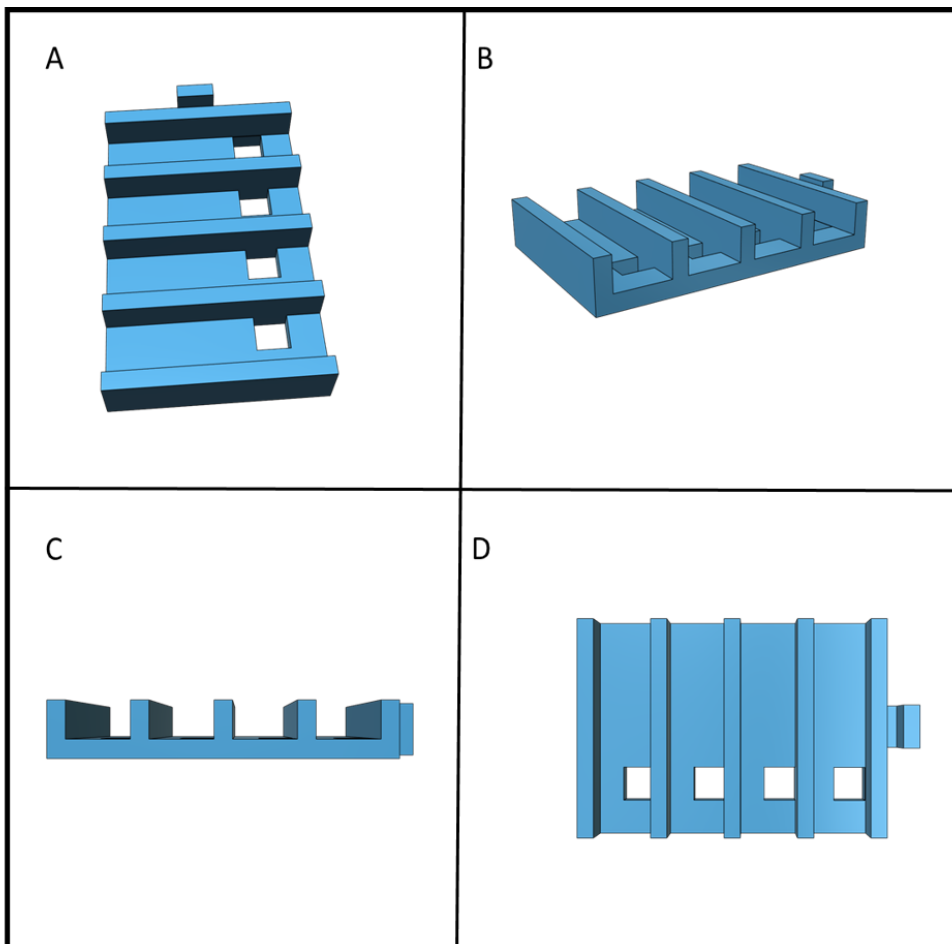


Figure 5: Hyperthermia administration platform, A. Orthotopic view B. Top-Left view, C. Front view, D. Top view.

The accessories utilized in the study (Figure 3 and Figure 4) were printed by Lulzbot Taz 5, 3D printer with Poly Lactic acid (PLA) plastic. For scaffold supporting during 3D printing of Isoflurane distribution nose cone (Figure 4) water soluble Polyvinyl alcohol (PVA) plastic was used.

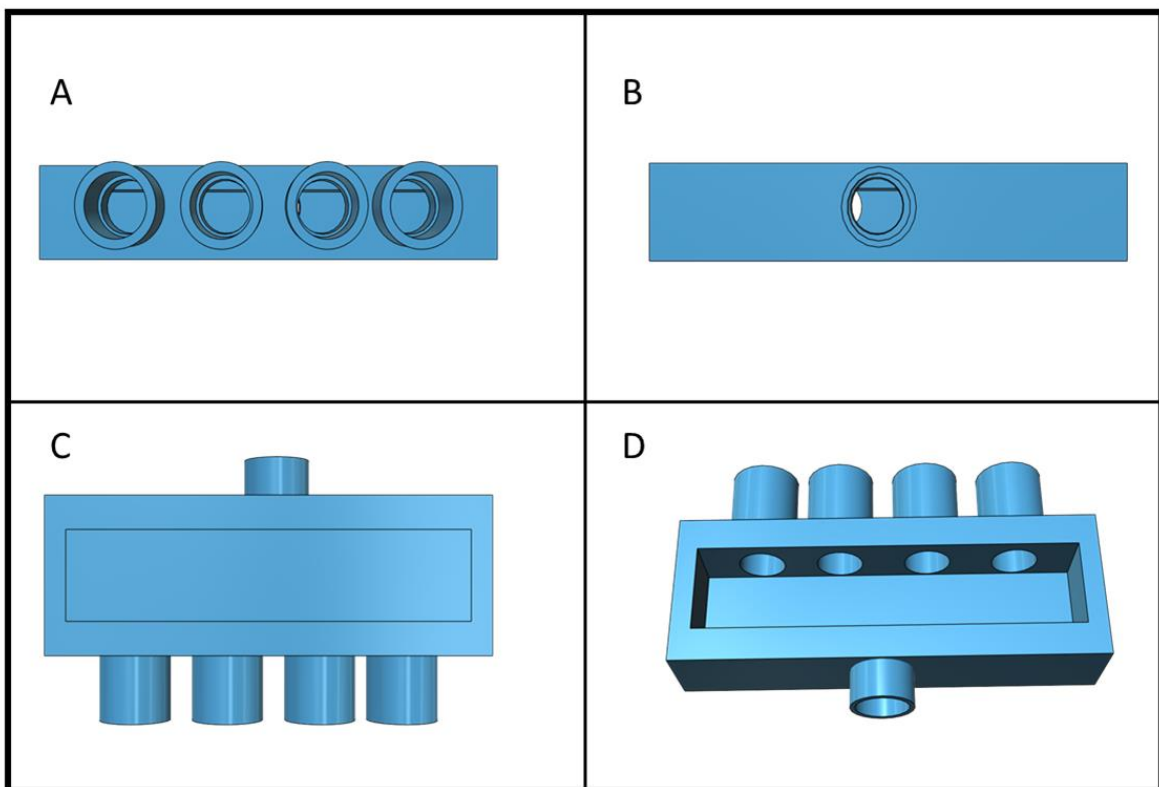


Figure 6: Isoflurane distribution nose cone, A. Front view B. Back view, C. Top view, D. Orthotopic Cross Section view.

3.2.Methods

3.2.1. Syngeneic Subcutaneous Tumor Model Development

3.2.1.1.Cell Culture

Pancreatic cancer cell line Panc02 of mouse origin was injected subcutaneously into the right or left flank of an 8-10 week old C57BL/6 mice from Charles Rivers Laboratories. The cells were cultured in McCoy's 5A High glucose complete media (Figure 5). The cells were grown in a tissue culture treated plates and passaged cells into P2-P5 passage numbers. The cell suspension for injection was prepared

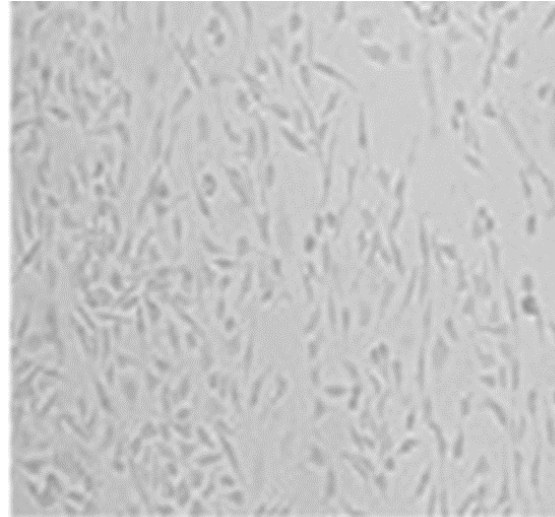


Figure 7: Mouse origin pancreatic cancer cell line (Panc02) cultured in 60mm Petri dish with McCoy's 5A high glucose complete media.

with Trypsin-EDTA (0.25%) containing 1×10^6 cells per injection with Matrigel in 1:1 ratio. The cultured cells were stocked with 10% Dimethyl sulfoxide (DMSO) at -80°C .

3.2.1.2.- Anesthetizing pre-injection

Isoflurane was the anesthetic employed to facilitate subcutaneous tumor inoculation into the mice. Animals were induced in an induction chamber with 2-4% isoflurane input along with oxygen at 1.5 L/min flow rate. After induction, they are moved to the

facemask with 1.5-4% isoflurane along with a 1.5L/min oxygen flow rate. Charcoal scavengers were attached to prevent the escape of unused anesthetic.

3.2.1.3. Subcutaneous Injection

The pancreatic cancer cells (Panc02) were injected subcutaneously, with a 25-28 gauge needle containing a volume of 100uL of pancreatic cancer cell suspension and Matrigel in 1:1 ratio. Use of 0.5 mL tuberculin syringes was preferred because of the absence of any dead-space. This specific needle will avoid the loss of any injectable while administering the injection. Before performing the subcutaneous injection, hair removal cream was used for removing hair from the site of injection and wiped clean with alcohol wipes. The needle was inserted into the subcutaneous space on the flank, and the contents were injected into the injection site. The injection into subcutaneous space was confirmed by observing the formation of a bulge just below the skin.

3.2.2. Tumor Volume Measurement

Tumor growth was assessed at least twice per week using calipers, preferably at the same time as body weight assessment to limit animal handling frequency. The length is defined as the longest dimension and width as the shortest dimension. The longest (L) and shortest (S) dimensions were determined with the calipers while the animal is held by scruffing. Tumor volume was be calculated using the following formula:

$$\text{Tumor Volume} = \frac{L \cdot S^2}{0.5}$$

3.2.3. Animal Monitoring

Mice inoculated with tumors and irradiated and undergoing treatment were observed daily in the cage to monitor morbidity and mortality for a maximum of 45 days post radiation therapy administration. The animals were observed for posture, gait, activity, malocclusions, and dermatitis according to the Fowler method (Table 1) for grading radiation reactions.

A veterinarian were notified for unexpected changes in health status including rectal prolapse, malocclusion, and dermatitis exceeding 1.5 (Fowler et al.) where a grade of 1.5 is equivalent to some breakdown of skin, scaly or crusty appearance, puffiness plus creases in the skin, and severe redness).

3.2.3.1. Body Weight Measurements

After tumor inoculation, animal body weights and tumor measurements were recorded at least twice per week during the in-life phase until the earliest predictive indicator of impending morbidity (e.g. body weight loss) in which case more frequent observations

was made. Animal body weight was recorded at the time the animal's identification is assigned, on the day of tumor inoculation.

3.2.3.2.Transport of Animals

When transporting the animals from their Animal Facility to a Laboratory (for irradiation, drug dosage or euthanasia), they were transported by placing their cages onto a wheeled cart. The cages were covered with a sheet or similar opaque draping to prevent visualization of the animals during transport.

3.2.3.3.Evaluation of rodent incisors:

Animals undergoing partial body irradiation (PBI) are likely to develop malocclusion or tooth decay during the in-life phase (Figure 6). The rodent was restrained by the scruffing method in a class II biosafety cabinet, to evaluate the signs of malocclusion or tooth decay. A sterile cotton swab was used to gently push back the lips of the animal to view the incisors and rostral gums (Leigue and Moore, 2016). The teeth were examined for proper alignment, good length, and correct occlusion according to the following guidelines approved by Veterinary Resources:

- a. Proper alignment: The teeth should grow near parallel to the vertical axis of the jaw

- b. Proper length: Visually check that the pair of the top incisors should be approximately 1/3-1/4 of the length of the lower incisors.
- c. Proper occlusion: The surface of the tooth that grinds against the opposite tooth should be near perpendicular to the long axis of the tooth. For instance, the shaft of the letter 'T' represents the long axis of the tooth, the top 'bar' of the capital 'T,' the occlusive surface wear pattern. Evaluate for tooth fracture or deflection preventing normal wear as teeth can later overgrow into the roof or tongue of the mouth or cut/tear the gums.
- d. Evaluate the rostral gums for signs of bleeding, tears or ulcers. Regular incisors are of proper alignment and length, and gums show no signs of cuts or ulcerations. Malocclusion occurs when teeth are overgrown due to abnormal alignment of the mandibular and maxillary incisors (Figure 6).

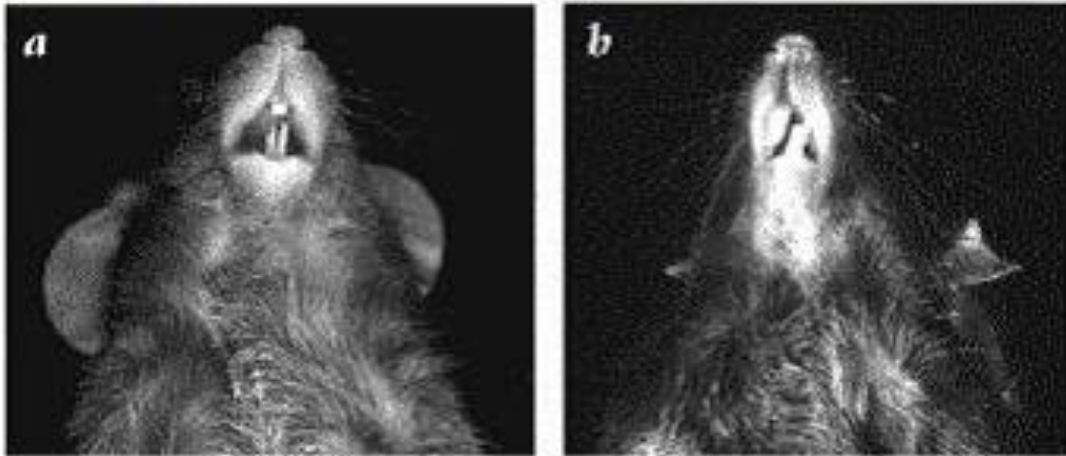
Maloccluded teeth may be clipped by restraining the animal using the scruffing method and gently clipping the edge of the tooth with surgical scissors disinfected in 70% alcohol.

Veterinary assistance was requested if any of the following are observed:

Figure 8: Normal vs. Maloccluded Rodent incisors

a) normal mouse incisors

b) maloccluded mouse incisors



- Short or fractured – one or more of the four incisors appear abnormally short.
- Thin – one or more of the four incisors appear unusually thin.
- Absent – one or more of the four incisors is missing.
- Ulceration/Abscess – area of eroded (open) epidermal tissues on gums, lips, or tongue; or infected closed sore appearing on the gums.

3.2.4. Hyperthermia Protocol

3.2.4.1. Anesthesia

Isoflurane was the anesthetic employed to facilitate subcutaneous tumor inoculation into the mice. Animals were induced in an induction chamber with 2-4% isoflurane input along with oxygen at 1.5 L/min flow rate. After induction, they are moved to the facemask with 1.5-4% isoflurane along with a 1.5L/min oxygen flow rate. Charcoal

scavengers are attached to prevent the escape of unused anesthetic. Ophthalmic ointment was applied to both eyes to protect the corneas from drying out.

They were monitored for any distress during the process of anesthesia, and thermal support was provided with a heating pad to maintain and prevent the significant drop in their body temperature. The animals were placed in a cage with ½ of the cage bottom on a thick towel or piece of cardboard and the other ½ of the cage bottom on a thermal supportive device. Animals are to be monitored until able to ambulate normally before return to their assigned husbandry rooms.

Maintenance of anesthesia was done using a customized 3D printed system that allows for continuous and uniform isoflurane gas (1-2 L/min O₂ with 2.0-4.0% isoflurane) exposure via nose cone while receiving hyperthermia treatment.

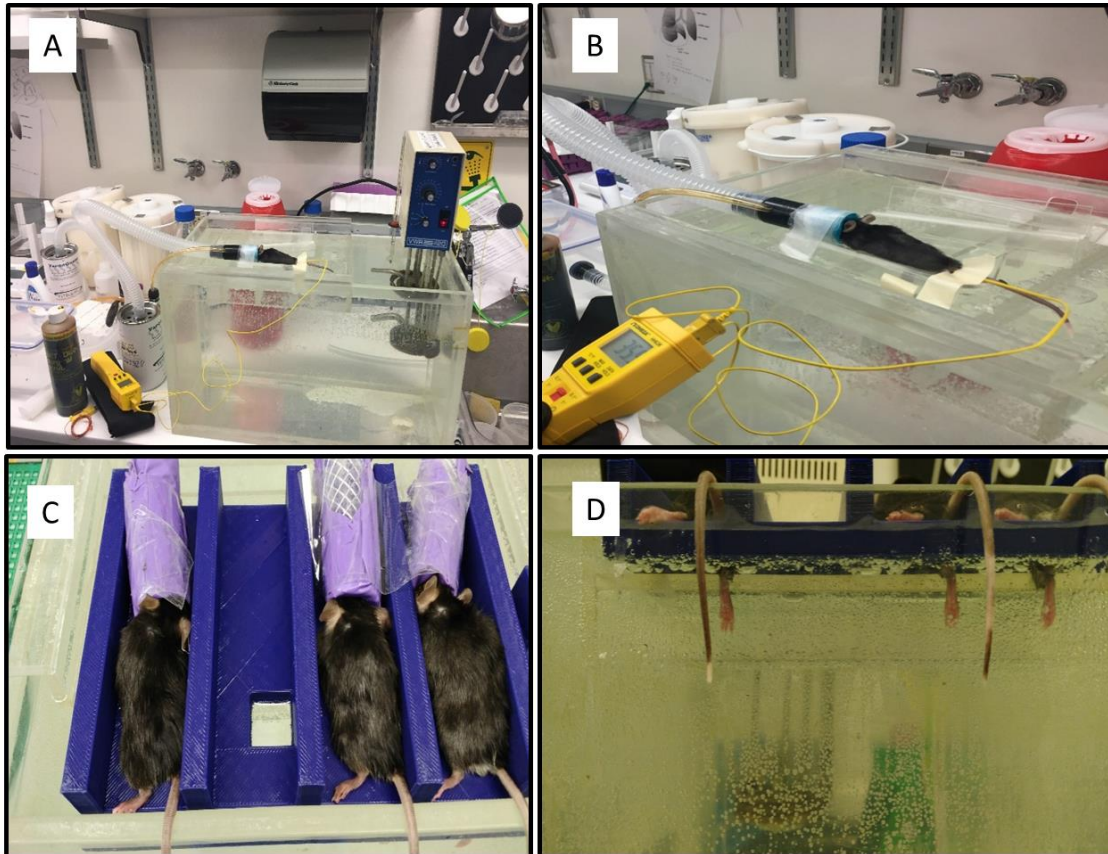


Figure 9: A. Water Bath setup with heating coil circulator and isoflurane vaporizer, B. Temperature thermocouple measuring water temperature, C. Mice under anesthesia receiving hyperthermia while laying on the 3D printed hyperthermia administration platform, D. Front view of mice legs immersed in the water bath during hyperthermia administration.

3.2.4.2. Hyperthermia Water bath

The water bath is filled with water, circulating water heater is set at 51°C to maintain water temperature at 42°C. The water temperature is configured to achieve core tumor temperature of 41.5°C in the subcutaneous tumor.

3.2.4.3.Hyperthermia Treatment Dosage

Once the mice are anesthetized, they were placed on the platform over the water bath and restrained to prevent significant movement and ensure a proper dosage of heat. The platform utilized was made of plastic (PLA) with minimal heat conduction to ensure heating of only the target region immersed in the water bath. Ophthalmic ointment was applied to both eyes to protect the corneas from drying out. The hind limb with the tumor was lowered into the water bath completely immersing the tumor in the heated water maintained at 42°C (confirmed and monitored with a standardized heat thermometer (Figure 7)). The limb of the mice was immersed in the water bath, and minimal exposure to the other regions was ensured. The mice were maintained at the set temperature for 30 minutes under close supervision to ensure a uniform and proper heat administration to the tumor.

The mice were monitored for the drop in body temperature and restraints were utilized to prevent the accidental drowning, non-targeted heating or overheating in the mice. The mice were carefully monitored for any signs of discomfort during the procedure, and appropriate steps were taken, veterinary consultation was considered in some cases. In the event of body temperature drop, thermal support was provided with a heating pad. The entire treatment was completed in no more than 60 minutes, after which thermal support was provided.

After successful administration of the heat to the tumor, the mice were transferred into their cages until the anesthetic wears off. Animals were dried off and then placed in a

clean cage with fresh bedding. Animals were monitored until able to ambulate normally before return to their assigned husbandry rooms. They were moved to their assigned cage after they awakened and observed for any issues. The hyperthermia treatment was administered on days 1, and three after being assigned to study groups

3.2.5. Radiation Protocol

3.2.5.1. Anesthesia

During imaging and irradiation, mice were anesthetized using isoflurane (Fluriso; pharmaceutical grade obtained through the VR). The induction of anesthesia was done by utilizing a precision vaporizer attached to a plastic chamber, exposing the animal to continuous isoflurane gas (1-2 L/min O₂ with 4.0-5.0% isoflurane). A charcoal scavenger was attached to protect personnel from waste gas. Maintenance of anesthesia was done using a customized system that allows for continuous isoflurane gas (1-2 L/min O₂ with 2.0-4.0% isoflurane) exposure via nose cone while inside the Small Animal Radiation Research Platform (SARRP) for imaging and irradiation.

A charcoal scavenger was attached to this system also to protect personnel from waste gas. Ophthalmic ointment was applied to both eyes to safeguard the corneas from drying out. During anesthesia recovery, the animal's cage was placed on a thermal supportive pad. The mice were put on the pad for recovery but were able to move off the heat once they are awake. The total time for tumor imaging and irradiation should

take approximately 20-30 minutes. If the mice were in the SARRP for longer than 20 minutes, thermal support was provided.

3.2.5.2.Pancreatic Tumor Imaging

Once the mice are anesthetized, they were placed stomach down and secured in place onto the animal platform of the SARRP. The nose cones of the isoflurane system were placed over the nose and mouth of the mice. The hindlimb region and the pelvic area of the mice were imaged using the SARRP's onboard CT scanner. The SARRP software will reconstruct a 3D picture of the area, and the tumor was identified. The center of the radiation field was placed in the center of the detected subcutaneous tumor.

3.2.5.3.Non-invasive imaging procedures (CT)

Some studies required non-invasive imaging procedures such as CT. All equipment used for non-invasive imaging computerized tomography (CT) were designated for small animals in preclinical research use. Hospital equipment was not be used for animals in this protocol

3.2.5.4. Animal CT Imaging

Depending on animal size, imaging was performed at low-medium (1.53) or medium (1.82) or medium high (2.28) or high (3.33) magnification settings, with the number of bed positions depending on animal length and technician's discretion. Data acquisition was nominally at 80kVp and 500uA for 180 angles over 360 degrees, though these parameters and the acquisition time per angle are user-adjustable. Image reconstruction with a modified Feld Kamp algorithm will typically take 3-4 minutes per bed position. Image resolution was between 15 and 200 microns depending on data acquisition and image reconstruction parameters, with greater image reconstruction times for higher resolution. Image acquisition and image reconstruction took between 0.5 and 2 hours depending on system options, with the highest resolution taking the longest time. Physiological monitoring of the respiratory signal was employed to aid in imaging at different phases of the respiratory cycle (i.e. full inhale/ end exhale).

3.2.5.5. Tumor Irradiation

After the isocenter of the radiation field is placed, a total dose of 8 Gy was delivered to the tumor. A collimator limited the X-ray field size to 20 mm X 20 mm, and four separate beam angles were used to minimize normal tissue damage (see Figure). The maximal energy used to generate the X-rays was 225kVp and 13mA. After irradiation, the mice were placed back into their cages to recover from anesthesia. Before each imaging and irradiation session, the animal platform was cleaned with 70% isopropyl alcohol, as well as after the last radiation session. The animals received two fractions

of 4 Gy radiation amounting to a total of 8 Gy dose, on days 1, and three after treatment initiation.

Irradiation lasts approximately 20-30 minutes depending on the total dose and dose-rate. Immediately after irradiation, animals were removed from the (Leigue and Moore, 2016) platform and placed on a thermostatically controlled, scientific grade, re-usable heating blanket. The heating blanket is placed under only half of the cage so that the animal may move out of the heat. Animals are continuously monitored until fully awake and mobile at which time they are placed back in the animal housing facility.

3.2.5.6.Supportive care

Although the radiation in our model specifically targets flank tumor, supportive care may sometimes be necessary for animals that have malocclusions or radiation-exacerbated dermatitis. All supportive care necessary was administered only after veterinary consultation.

3.2.6. Immunotherapeutic Treatment

Anti-mouse OX40 monoclonal antibody was purchased from suppliers (BioXcell) and stored until use according to manufacturer's storage instructions. The monoclonal antibody was prepared and administered according to the study timeline. The mice were

restrained by scruffing, and the abdominal region was exposed. A 200ug/mice dose of the monoclonal antibody was prepared in a syringe and injected intraperitoneally into the mice.

The syringe needle was inserted into the intraperitoneal cavity, and then the syringe piston is pulled back a little to ensure that the syringe is in the intraperitoneal cavity (confirmed by the absence of blood or urine when the piston is drawn back).

The first injection will be administered on the day of first radiation dosage and after that administered every five days two more times. The dosage of the monoclonal antibody will be carried out on days 3, 8, and 13 after the randomization of the mice into the study. The animals will regularly be monitored by the animal monitoring guidelines set forth by the Institutional Animal Care and Use Committee (IACUC) at the University of Maryland, Baltimore.

3.2.6.1. Drug Preparation

The OX-40 monoclonal antibody is available as a concentrated antibody stock solution. The stock solution is diluted with saline (pH=7.4) to a concentration of 2ug/ul. The prepared drug will be stored at 2-8°C before administration for a maximum of 48 hours. The monoclonal antibody had no known side effects and was well tolerated when administered in monkeys and humans. The drug is not available commercially in

pharmaceutical grade. The injections will be administered based on the volume for a calculated dosage of 200ug/mice.

3.2.6.2. Intraperitoneal (I.P) injection

The test article was administered using a 50cc Tuberculin syringe with a 27.5 gauge needle. Before the drug is delivered, the injection site is wiped with alcohol prep pad. Animals are restrained by hand using scruffing or the tail wrap method. Scruffing involves the grasping of the rump (at the tail) firmly between the 4th and 5th fingers and the neck with the thumb and index fingers. Animals are held firmly, but gently. The injection site is wiped with alcohol prep pad. The body is tilted at a 10-15 degree angle, and back support is provided as the article is injected I.P. into the right lower quadrant. Test articles were prepared with aseptic technique.

3.2.7. Euthanasia Criteria and Graphical depiction

Animals will be euthanized accordingly at their study end points (10 and 45 days after randomization into the study). Alternatively, animals were also euthanized when the animals demonstrated signs of morbidity or lose more than 20% of the maximum body weight. Also, the animals were also euthanized when the tumor burden exceeded the IACUC approved guidelines, of tumor dimension extending beyond 1.5 cm in any direction of measurement with a Vernier caliper. The mice euthanasia data was plotted

on a Kaplan-Meier survival plot to demonstrate the survivability of each treatment. This depiction primarily depicts the lack of toxicity due to any treatment strategy employed during the study and in no way represents the increased survival statistics due to the treatment plans.

3.2.8. Flow Cytometry

3.2.8.1. Organ processing

3.2.8.1.1. Processing tumor

Collect the tumors in the 40um cell strainer. Mash with a plunger to create a cell suspension on a plate. Pipette in a few ml of RPMI containing 10% FBS and then collect the cell suspension into a 50ml tube. Spin down at 2000rpm, 5min, and low brake. Resuspend in 1XPBS + 2%FBS and count the cells.

3.2.8.1.2. Processing blood

Collect in 15ml tube 100ul of blood. Add 2 ml of 1X RBC lysis buffer (Thermo-Fischer Scientific) and incubate for 10min at RT. Neutralize the reaction with 2 ml of RPMI+10%FBS. Spin the cells down and resuspend in 1X PBS+2%FBS to count the cells.

3.2.8.2. Staining Protocol

Add 1×10^6 cells into each FACS centrifugation tube. Add 1X PBS + 2% FBS buffer containing different antibodies (1:1-1:3). Incubate at 4°C for one hour. Run FACS the same day.

3.2.8.3. Fixing Sample after Staining

To set the stained specimens, add 4% paraformaldehyde for 10-20 minutes to the cells. Run FACS within 3-7 days.

3.2.8.4. Flow Cytometry Analysis

To analyze flow cytometry sample, prepare the BD LSRII flow cytometer by washing with 2% contrad and double distilled water. The samples were vortexed before loading the sample, acquire after loading and record the data. Label the stored flow cytometry data accordingly. Export the data as an experiment and as individual sample FCS files. Analyze the data with Flow Jo or FCS Express. The gating was performed by using negative control and isotype controls to subtract the background population. The compensation for the dyes was performed on Flow Jo at the time of data acquisition.

3.2.9. Statistical Analysis

The statistics were analyzed by Student t-test, one-way ANOVA, two-way ANOVA and correlation analysis by Microsoft Excel or IBM SPSS. Graph Pad Prism software was used to plot the analyzed data.

4. Results

4.1. Tumor Regression Study

4.1.1. Tumor Survival

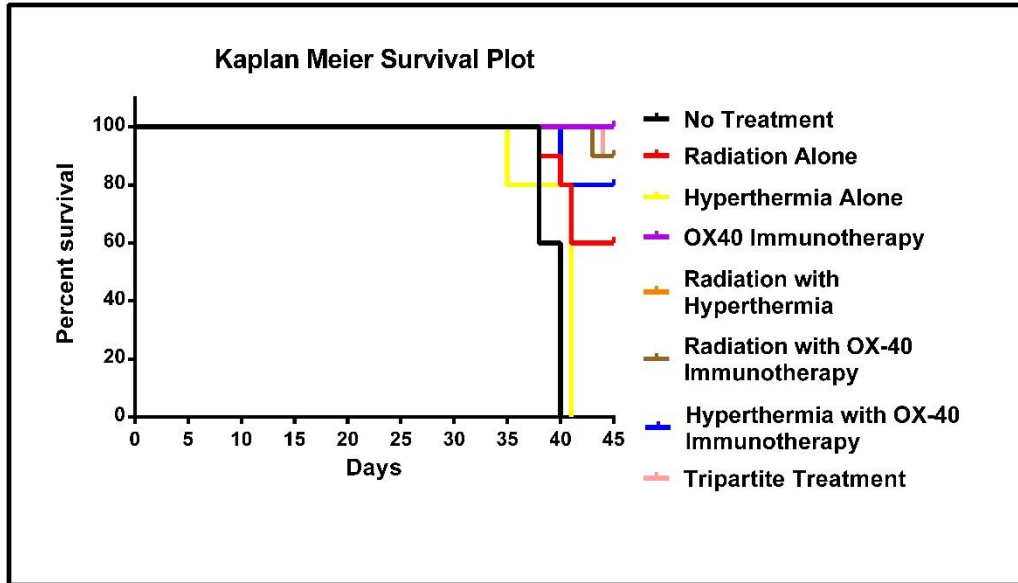


Figure 10: Survival data for eight different treatment groups demonstrating survival percentage of mice with 10 animals per treatment group.

4.1.2. Body Weight

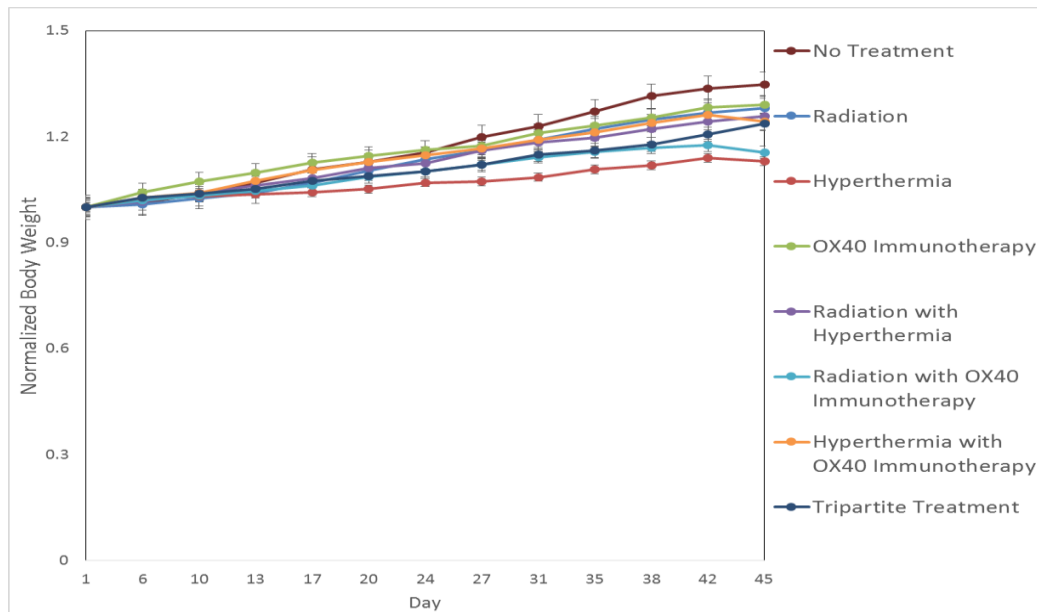


Figure 11: Body weight (grams) distribution for each eight different treatment group (n=10); 'n' demonstrates number of animals per group (each point demonstrates mean \pm standard error of mean (SEM)).

4.1.3. Tumor Volume Regression

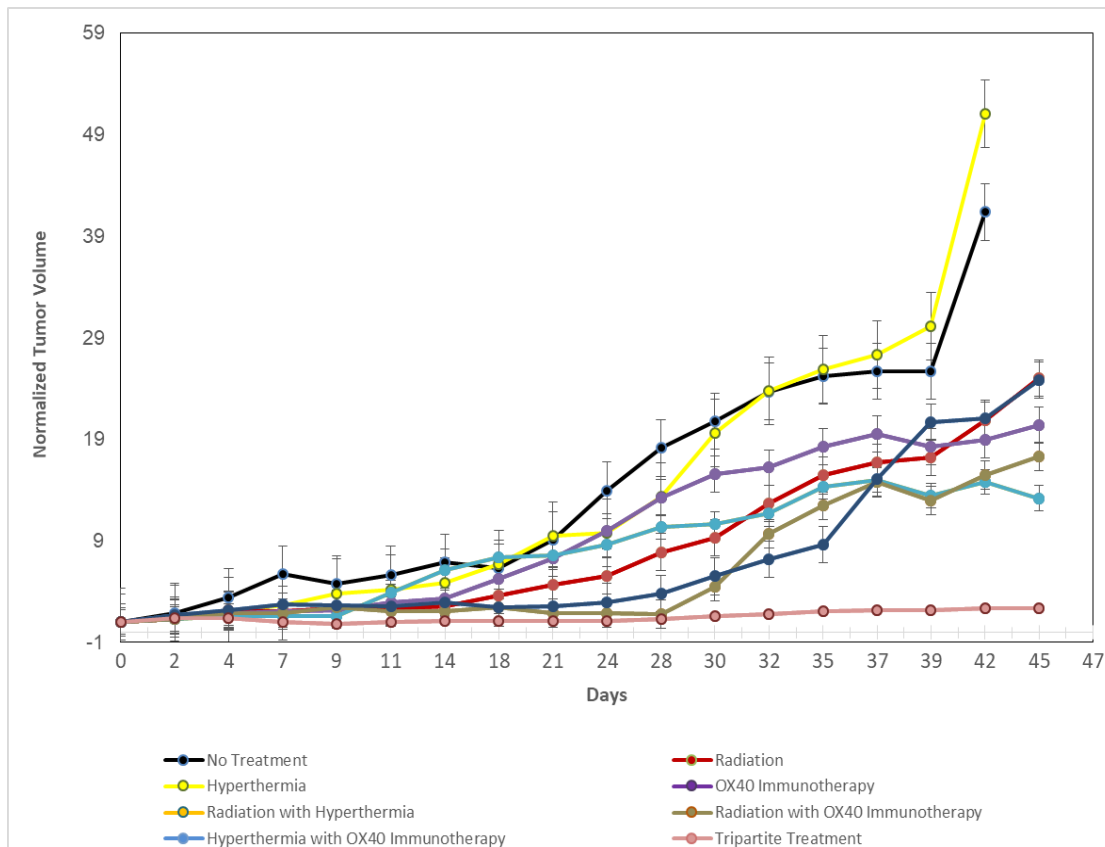


Figure 12: Normalized tumor volume (mm³) distribution among eight different treatment groups (n=10); 'n' demonstrates number of animals per group (each point demonstrates mean \pm standard error of mean (SEM)). Statistics done by student's t-test.

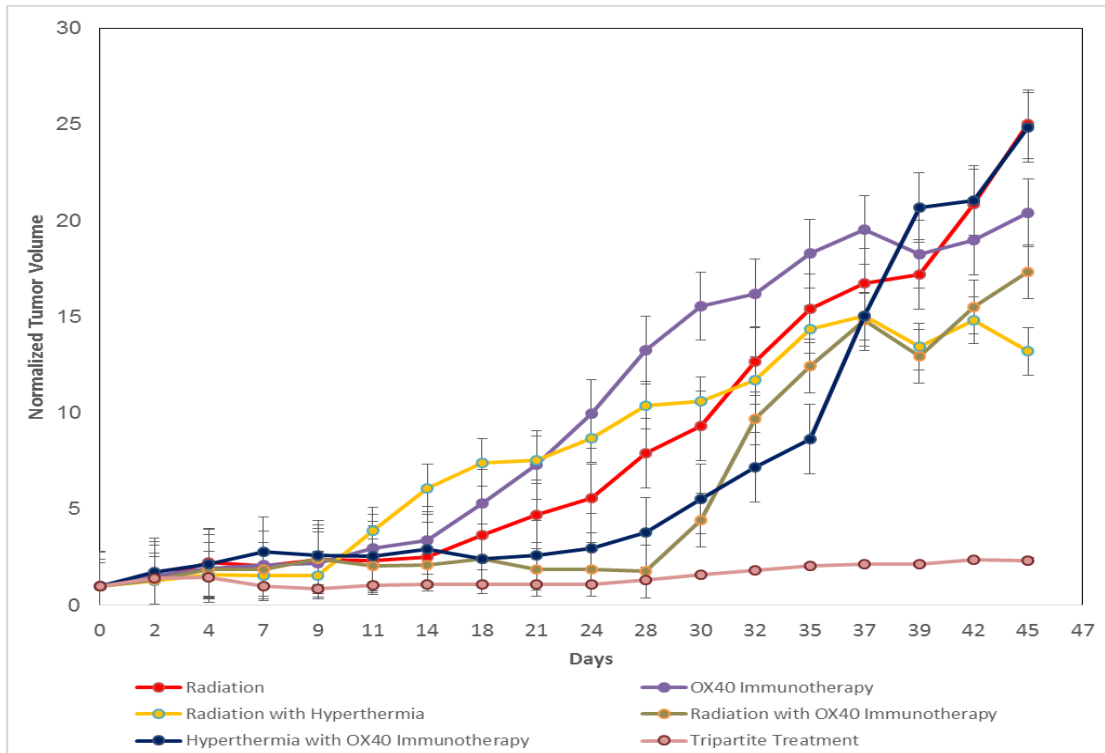


Figure 13: Normalized tumor volume (mm³) distribution between combination therapy and tripartite treatment (n=10); 'n' demonstrates number of animals per group (each point demonstrates mean ± standard error of mean (SEM)). Statistics done by student's t-test.

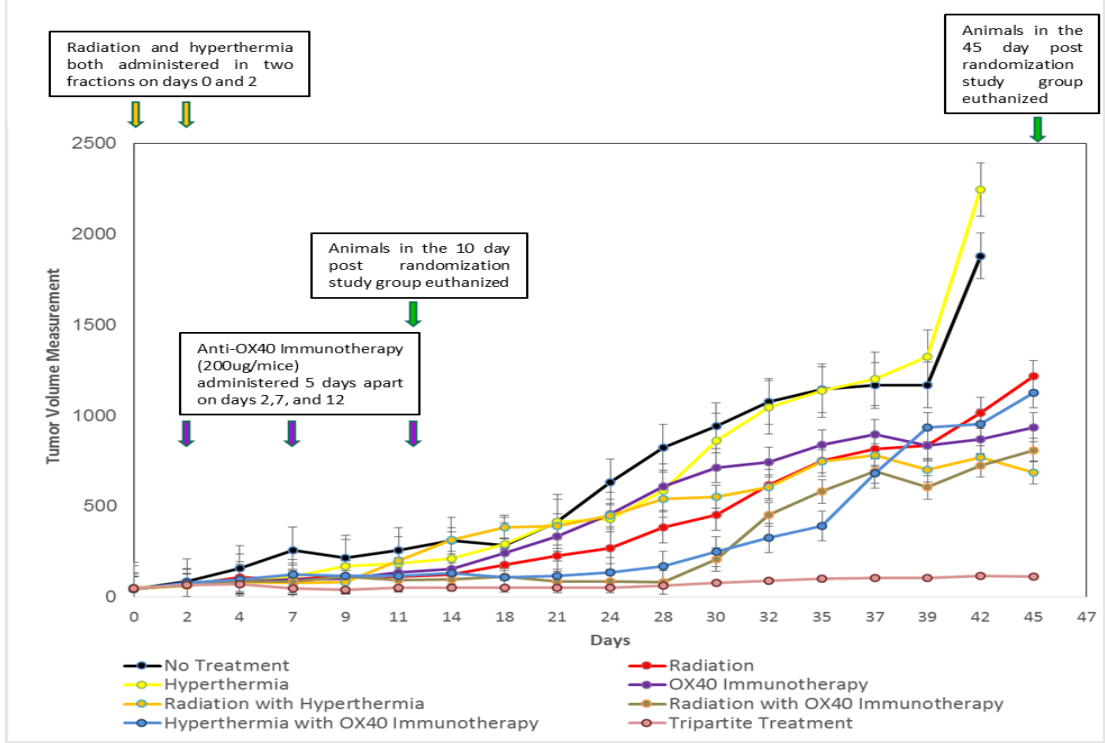


Figure 14: Tumor volume (mm³) distribution among eight different treatment groups (n=10); 'n' demonstrates number of animals per group (each point demonstrates mean ± SEM). Arrows demonstrate the treatment and euthanasia time points. Statistics done by student's t-test.

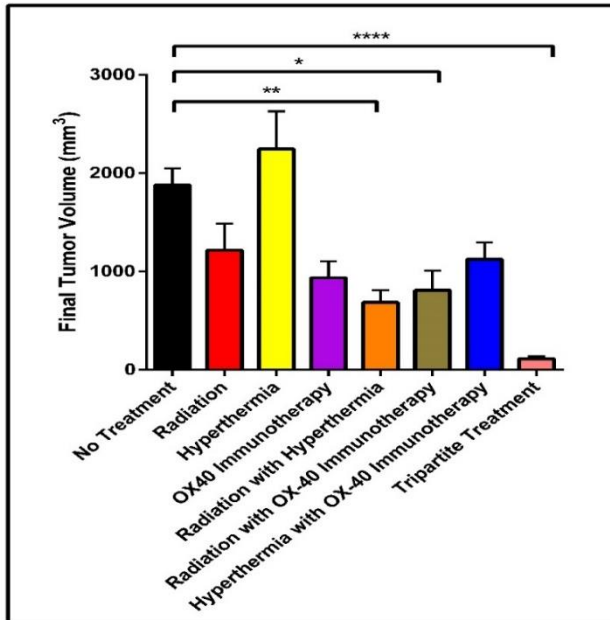


Figure 15: Histogram demonstrating the difference in tumor volume between the study groups (n=10), 'n' demonstrates number of animals per group (mean \pm SEM). * $p < 0.05$, ** $p < 0.01$, **** $p < 0.0001$. Statistics done by student's t-test.

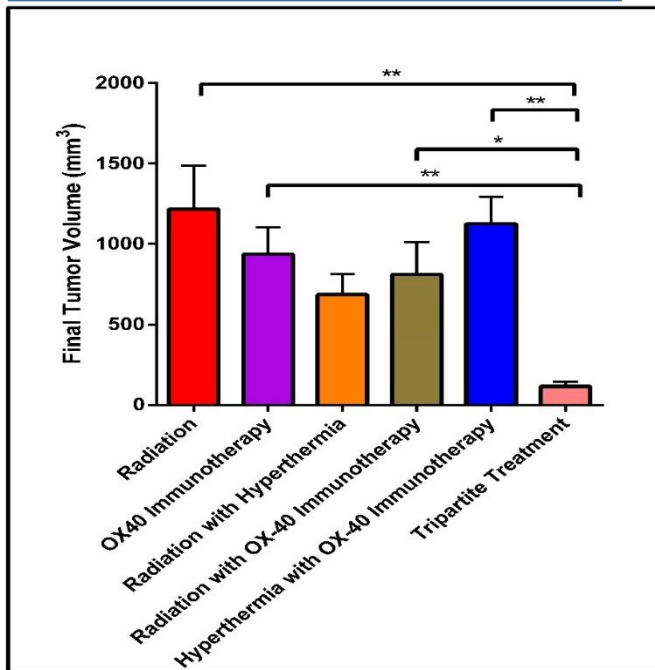


Figure 16: Histogram demonstrating the difference in tumor volume between the group of animals treated with radiation versus the combination of the treatments (n=10), 'n' demonstrates number of animals per group (mean \pm SEM). * $p < 0.05$, ** $p < 0.01$, **** $p < 0.0001$. Statistics done by student's t-test.

4.2. Immunological Analysis

4.2.1. Flow Cytometry

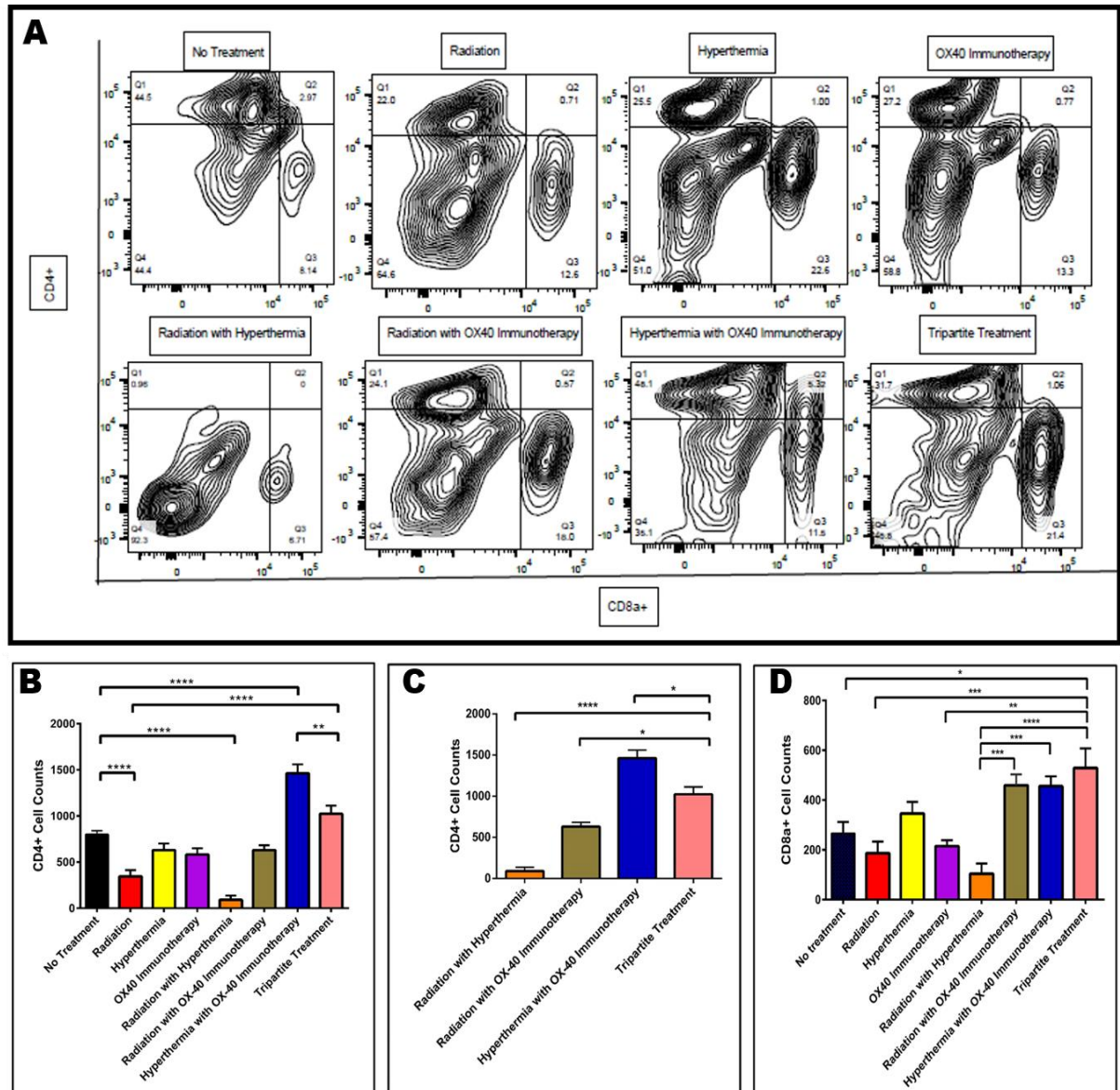


Figure 17: (A) Representative contour plot flow cytometry analysis for CD4 versus CD8a cell population of tumor from all different treatment group from animals euthanized 10 days after randomization into the study treatment group; (B) Histogram depicting the count of CD4+ cells among the total number of WBCs analyzed between different treatment groups (mean \pm SEM) ; (C) Histogram depicting the count of CD4+ cells among the total number of WBCs analyzed between the combination treatment groups (mean \pm SEM); (D) Histogram depicting the count of CD8a+ cells among the total number of WBCs analyzed between different treatment groups (mean \pm SEM). * $p < 0.05$, ** $p < 0.01$, *** $p < 0.001$, **** $p < 0.0001$. Statistics done by student's t-test.

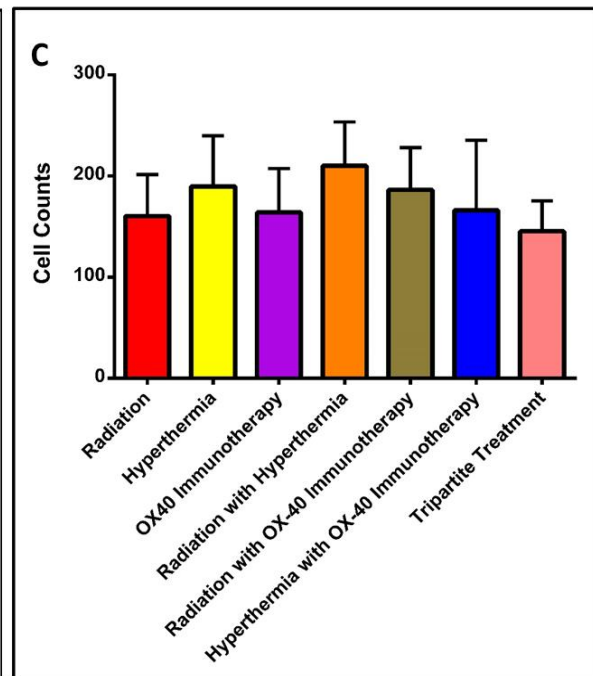
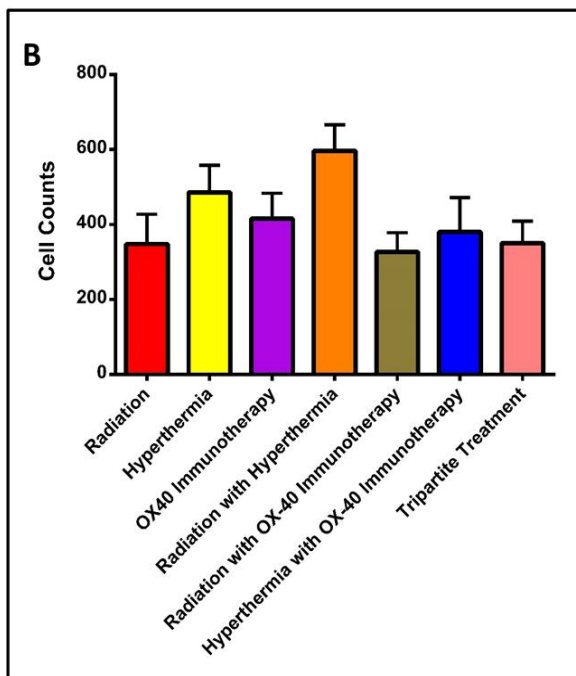
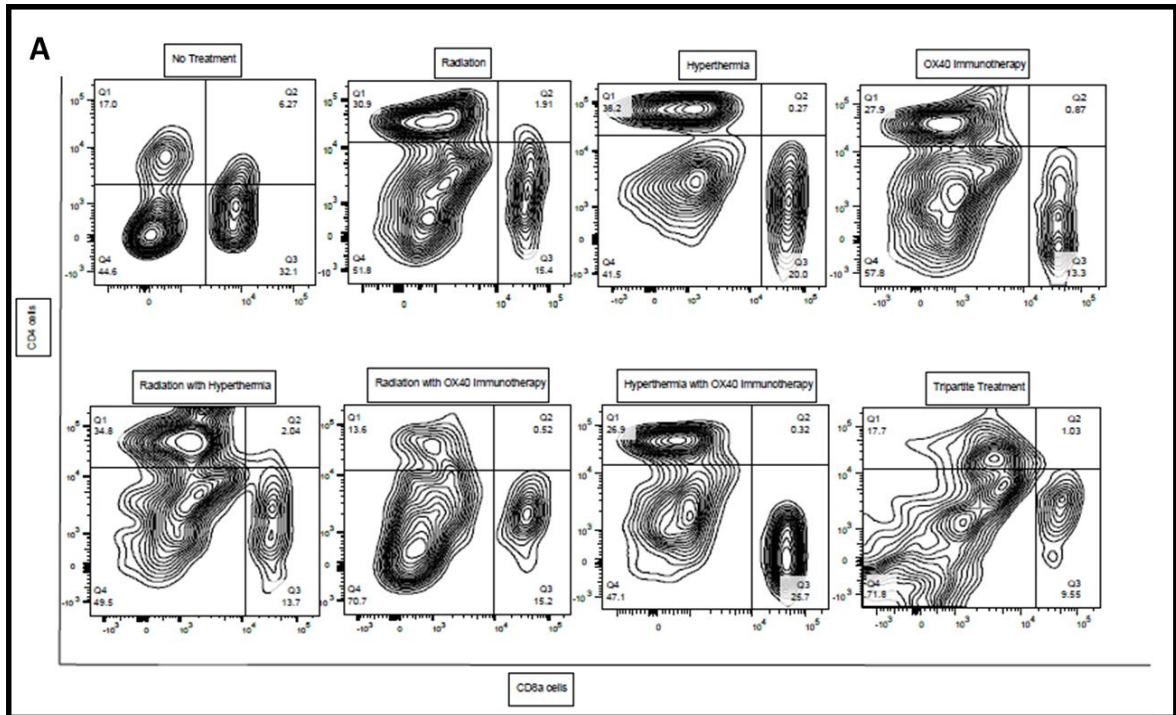


Figure 18: (A) Representative contour plot flow cytometry analysis for CD4 versus CD8a cell population of tumor from all different treatment group from animals euthanized 45 days after randomization into the study treatment group; (B) Histogram depicting the count of CD4+ cells among the total number of WBCs analyzed between different treatment groups (mean \pm SEM); (C) Histogram depicting the count of CD8a+ cells among the total number of WBCs analyzed between the combination treatment groups (mean \pm SEM). No statistical significance was observed. Statistics done by student's t-test.

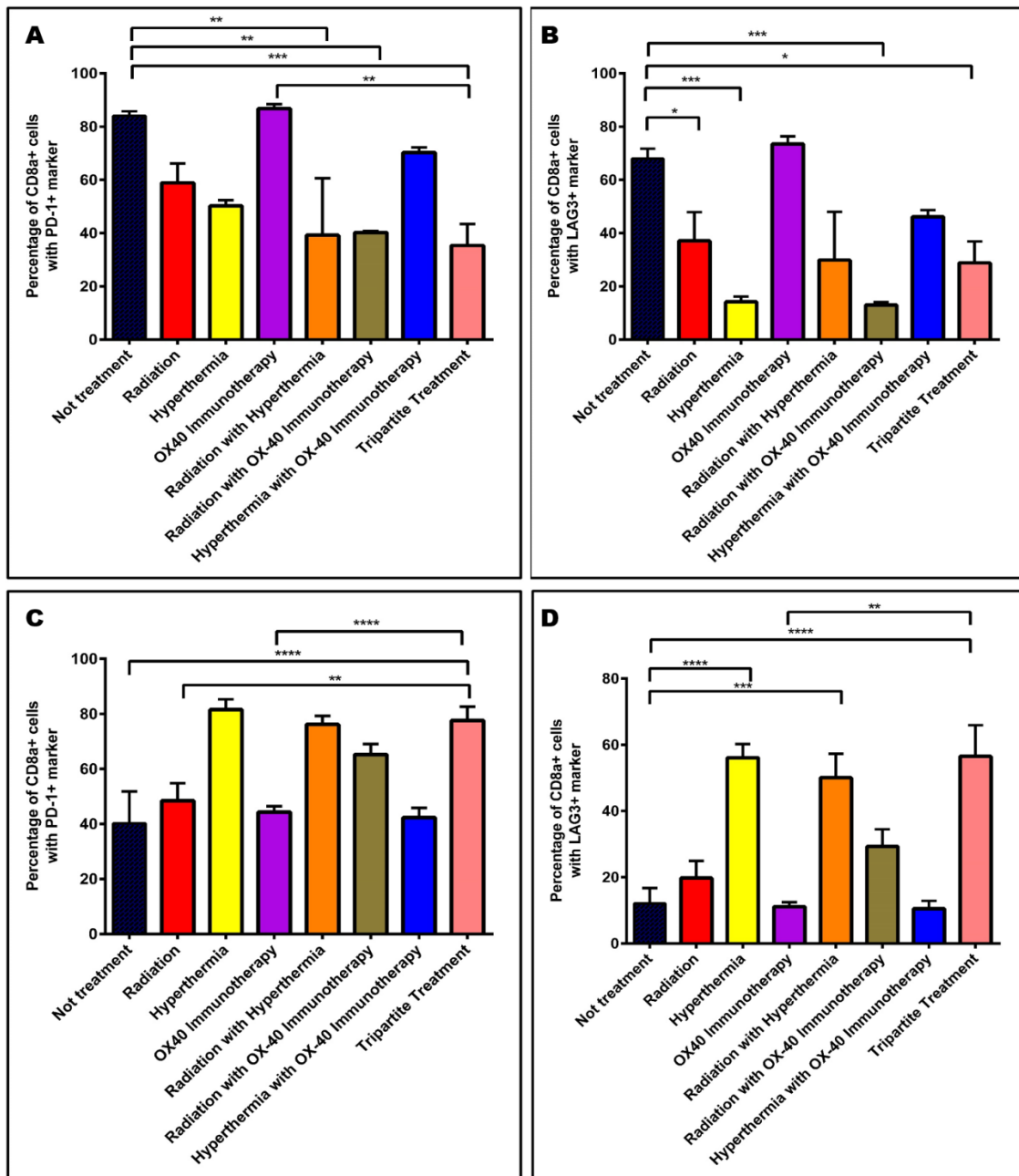


Figure 19: (A) Histogram depicting the cell count of CD8a+PD-1+ cells among the total number of WBCs in the tumor of animals euthanized 10 days after randomization into study groups; (B) Histogram depicting the cell count of PD-1+LAG3+ cells among the total number of WBCs in the tumor of animals euthanized 10 days after randomization into study groups (mean \pm SEM); (C) Histogram depicting the cell count of CD8a+PD-1+ cells among the total number of WBCs in the tumor of animals euthanized 45 days after randomization into study groups (mean \pm SEM); (D) Histogram depicting the cell count of PD-1+LAG3+ cells among the total number of WBCs in the tumor of animals euthanized 45 days after randomization into study groups (mean \pm SEM). * $p < 0.05$, ** $p < 0.01$, *** $p < 0.001$, **** $p < 0.0001$. Statistics done by student's t-test.

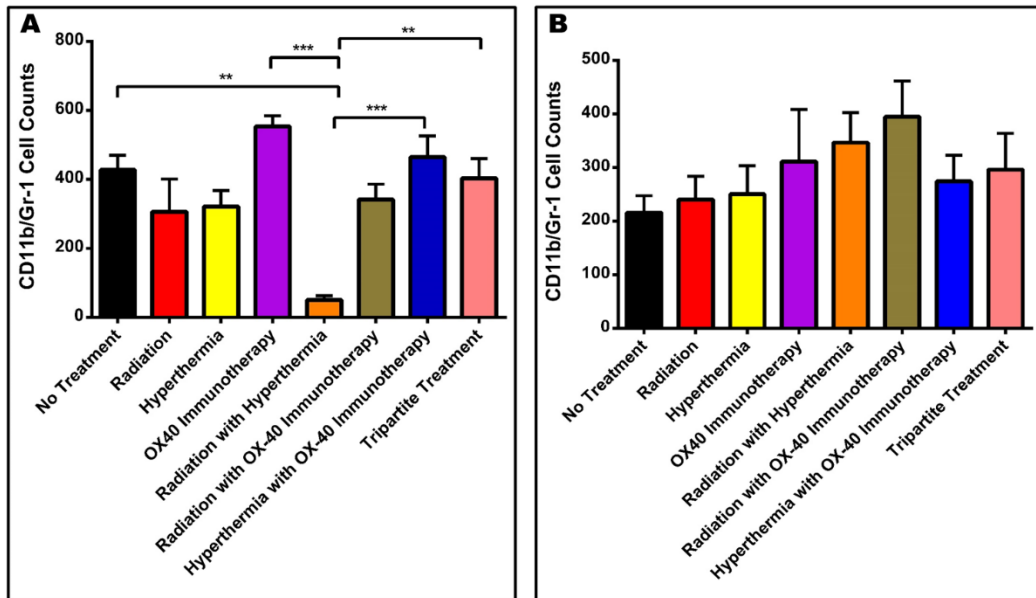


Figure 20: (A) Histogram depicting the cell count of CD11b/Gr-1 double positive cells among the total number of WBCs in the tumor of animals euthanized 10 days after randomization into study groups (mean \pm SEM); (B) Histogram depicting the cell count of CD11b/Gr-1 double positive cells among the total number of WBCs in the tumor of animals euthanized 45 days after randomization into study groups (mean \pm SEM); ** $p < 0.01$, *** $p < 0.001$. Statistics done by student's t-test.

5. Discussion

5.1. Tumor Growth Delay

Pancreatic cancer is the fourth most deadly cancer in the United States, with a five-year survival rate of a measly 7.7% (Siegel, Miller and Jemal, 2017). The therapy with the tripartite treatment of radiation, hyperthermia and anti OX40 drug, demonstrated a significantly higher reduction in tumor volume compared to no treatment study group. The animal receiving no treatment showed an increase in the normalized tumor volume by 41.4 ± 5.2 (mean \pm standard deviation) fold, compared to 2.3 ± 1.7 in the animals receiving the tripartite treated. This outcome is the most desired outcome with tumor regression at its peak, and minimal relapse was observed (Figure 12). The tumor growth delay noted in the mice receiving the tripartite treatment was evaluated for statistical significance by one-way ANOVA coupled with multiple comparisons Tukey's analysis of the column means, which demonstrated a p value of less than 0.0001 when compared to the animals with subcutaneous pancreatic tumors receiving no treatment (Figure 15).

In addition to the anti-tumor effect of the tripartite treatment observed by the comparison of normalized tumor volume, the volume of the subcutaneous tumor also demonstrated the same growth delay and statistical significance (Figure 14). The changes in the tumor growth rate and potential tumor growth delay is illustrated by line plots generated through Microsoft Excel (Figure 12, Figure 13, and Figure 14). Furthermore when compared to the effect of the radiation therapy; one of the standards of care treatment, the tripartite treatment demonstrated a significantly ($p < 0.01$) higher inhibition of tumor growth (Figure 14).

The treatment of the subcutaneous pancreatic cancer by individual therapeutic regimens yielded positive outcomes, but no treatment showed statistical significance ($p > 0.05$) (Figure 15). Radiation therapy alone demonstrated a final tumor volume fold increase of 25.0 ± 13.6 (Original Tumor Volume: $1217.5 \pm 661.1 \text{ mm}^3$), while immunotherapy treatment by anti-OX40 had a final tumor volume fold change of 20.4 ± 11.5 ($937.0 \pm 525.7 \text{ mm}^3$). In comparison, the difference in the effect of the radiation therapy and anti-OX40 immunotherapy was not statistically significant (Figure 13 and Figure 14).

In contrast treatment with hyperthermia alone aggravated the tumor growth demonstrating a final tumor volume fold change of 51.1 ± 24.6 ($2246.8 \pm 1081.3 \text{ mm}^3$), which is significantly larger in tumor volume compare to the animals receiving radiation alone ($p < 0.05$) and OX40 immunotherapy ($p < 0.001$). To further understand the effect of combining individual treatments we treated each of these three different treatments in combination with another. The combination of treatments led to three different treatment groups of combination therapy, not inclusive of the tripartite treatment group (Figure 12, Figure 14, and Figure 13).

The treatment of the pancreatic tumor with a combination of radiation therapy and hyperthermia had an average final tumor volume fold change of 13.2 ± 7.6 ($687.0 \pm 397.9 \text{ mm}^3$). In comparison, the average final tumor volume fold change in mice receiving a combination of radiation and anti-OX40 immunotherapy was 17.3 ± 13.6 ($810.8 \pm 636.5 \text{ mm}^3$) (Figure 13, Figure 14, and Figure 16). The statistical analysis of

these treatments demonstrated no statistical significance when compared to animals receiving only radiation therapy.

Also among mice receiving a combination of hyperthermia and anti-OX40 immunotherapy, the average normalized tumor volume was 24.8 ± 10.6 similar to the outcome observed in the mice receiving this treatment individually. The difference in the outcome when compared to the no treatment group is statistically significant in all treatment groups except the hyperthermia alone group. (Figure 15 and Figure 16). Though combination therapy usually yields better results in comparison to individual treatment, the combination therapy by hyperthermia in conjunction with anti-OX40 immunotherapy led to no improvement in overall tumor growth delay outcome. When compared to radiation therapy alone group, which is one of the standard of care therapeutic strategies employed in the treatment of pancreatic cancer patients in the clinic hyperthermia with anti-OX40 yielded no superior outcome. In support, the final tumor weight also demonstrated a similar trend in significant ($p < 0.01$) tumor growth inhibition between the tripartite treatment and no treatment groups (Supplementary Figure 1) Interestingly after the completion of treatment on day 12 of the study the tumors start re-growing from as early as day 17 and therefore, continuation of immunotherapy treatment throughout the entire study must be considered as a viable treatment option for continued treatment response.

Following the evaluation of the tumor growth delay effect of the tripartite treatment, it became crucial to determine if any of the treatments in the study demonstrated increased survival. This analysis will help elucidate if any of the treatment strategies lead to

toxicity. The administration of hyperthermia resulted in the aggravation of the tumor growth rate and increased morbidity in the animals; this is demonstrated by 20% deaths by day 35 out of 45 days after randomization into the study. Also, a 100% mortality was observed in these animals by day 42 (Figure 10).

Among animals with subcutaneous pancreatic cancer receiving no treatment a 40% mortality was observed before day 42, while all the remaining animals were euthanized by day 42 by the IACUC guidelines for tumor size endpoint and morbidity. All treatment groups demonstrated mortality, except in the animals receiving anti-OX0 immunotherapy alone. In animals receiving only anti-OX40 therapy, no mortality was observed throughout the course of the study (Figure 10).

In contrast to our excellent tumor regression outcome, the survival percent of animals receiving the tripartite treatment was 90%. However, no signs of morbidity or body weight loss of no more than 20% were observed in that mouse (Figure 11). Also, no mice in the study demonstrated more than 20% of body weight loss throughout the course of the study. Furthermore, animals receiving a combination of hyperthermia with anti-OX40 immunotherapy showed a 20% mortality before day 40 in the study (Figure 10).

5.2.Flow Cytometric Analysis

The promising tumor growth delay results warranted the investigation of the role of immune system in the treatment of the pancreatic tumor. In flow cytometric analysis of

the tumor, digest revealed an increased population of CD4+ cells in the tumor microenvironment compared to all individual treatment groups. While comparing the animals treated with radiation therapy alone and tripartite treated animals a significant increase in the CD4+ cells was recorded in the 10-day study endpoint group animals ($p < 0.0001$). Similarly a statistically significant ($p < 0.01$) difference in the CD4+ cell count between anti-OX40 immunotherapy treated animals and the tripartite treated animals (Figure 17A, Figure 17B and Figure 17C).

Also, the tripartite treated mice demonstrated a significantly ($p < 0.0001$) higher CD4+ cell population compared to the radiation with hyperthermia group animals (Figure 17A and Figure 17B). To further solidify the anti-tumor effect of tripartite treatment the CD8a+ cytotoxic effector T- lymphocyte expression was evaluated. CD8a is a T cell marker expressed in effector T-lymphocytes. In animals receiving tripartite treatment demonstrated a significantly ($p < 0.001$) higher CD8a cells in the tumor microenvironment compared to the animals receiving radiation therapy only. The treatment with anti-OX40 drug also demonstrated significantly ($p < 0.01$) lower CD8a+ cell count compared to the tripartite treatment (Figure 17A, and Figure 17D).

In contrast, flow cytometric analysis of the animals from the 45-day study endpoint, none of the study groups demonstrated any statistically significant ($p > 0.05$) changes in the presence of T helper cells (CD4+) or effector T cells (CD8a+) cells. However, there was a presence of WBCs in the tumor microenvironment which was demonstrated by flow cytometric analysis of CD4+ and CD8a+ cells in the tumor tissue digest. All the animals in one of the treatment groups showed a distinguishable increase in the CD4

and CD8a population in the tumor microenvironment compared to the no treatment group animals. However, no statistically significant difference could be established in the target cell count among the different treat groups. This is in accordance with the initial hypothesis suggesting a decrease in the immune response over a period (Figure 18A, Figure 18B, and Figure 18C).

Furthermore, analysis of CD279 (PD-1) cells was performed to evaluate the immune suppressive effects of the Programed Death receptor (PD-1). In previous studies, PD-1 positive cells exhibit an immune inhibitory effect on CD8a+ T-lymphocytes and natural killer (NK) cells. Among animals in the 10-day study endpoint group significantly lower population of PD-1(CD279), positive cells compared to all the other treatment groups and no treatment group (Radiation versus Tripartite treatment-^{**} $p < 0.01$). This is indicative of and in support of the immune suppressive environment in pancreatic tumors (Figure 19A). However, in tumor 45 days study endpoint, the expression of PD-1 marker increased significantly ($p < 0.0001$) in the tripartite treated animals, marking this observation an excellent target for ultimate combination with anti PD-1 immunotherapy (Figure 19C).

Similarly, no statistically significant changes in the CD11b+/Gr-1+ Myeloid-derived suppressor cells (MDSCs) cell population was observed in the tripartite treated mice compared to no treatment group animals (Figure 20A). However interestingly combination of radiation and hyperthermia demonstrated a significant ($p < 0.01$) decrease in the MDSC population in the tumor compared all the combination treatment groups and the no treatment group (Figure 20A). In comparison, the animals in the 45-day group did not demonstrate any statistically significant difference in the

CD11b+/Gr-1+ cell in the tumor microenvironment. However no significant difference between the MDSCs immune microenvironment in tumor even 10-day and 45-day post randomization between any other treatment groups in the study (Figure 20A and Figure 20B).

The expression of Leukocyte Activation Gene (LAG3) has been associated with immunosuppression and activation of dendritic cells to mature dendritic cells, making it a crucial factor for analysis in a tumor microenvironment. Dendritic cells are key factors influencing the antigen presentation and activation of the helper T cells and cytotoxic T cells. In animals receiving the tripartite treatment a significantly ($p < 0.05$) higher cell population of LAG3 (CD223) + cells in the tumor microenvironment compared to the animals in the radiation therapy group. This is also in accordance with the initial hypothesis suggesting an increased infiltration and antigen presentation of the immune cells in the tumor (Figure 19B). Also similar to the 45-day observation for PD-1 marker, LAG3 also demonstrated a significantly ($p < 0.0001$) higher expression in tripartite treated animals indicative of the increased expression of mature dendritic cells crucial for enhanced antigen presentation and thereby T cell activation (Figure 19D).

6. Conclusion

In conclusion, the tripartite treatment by fractionated radiation therapy, hyperthermia, and anti-OX40 immunotherapy treatment demonstrated a significant tumor growth delay compare to animals in the other study groups. Though the administration of each treatment regimen led to tumor growth delay no other treatment strategy investigated

in the study demonstrated as significant an impact on the tumor growth delay as the tripartite treatment. Also, we were able to prove a connection between the tripartite treatment and its immunological response contributing to the increased cytotoxic effect in pancreatic tumors and antigen presenting dendritic cell population in the tumor microenvironment.

7. Future Directions and Potential Caveats

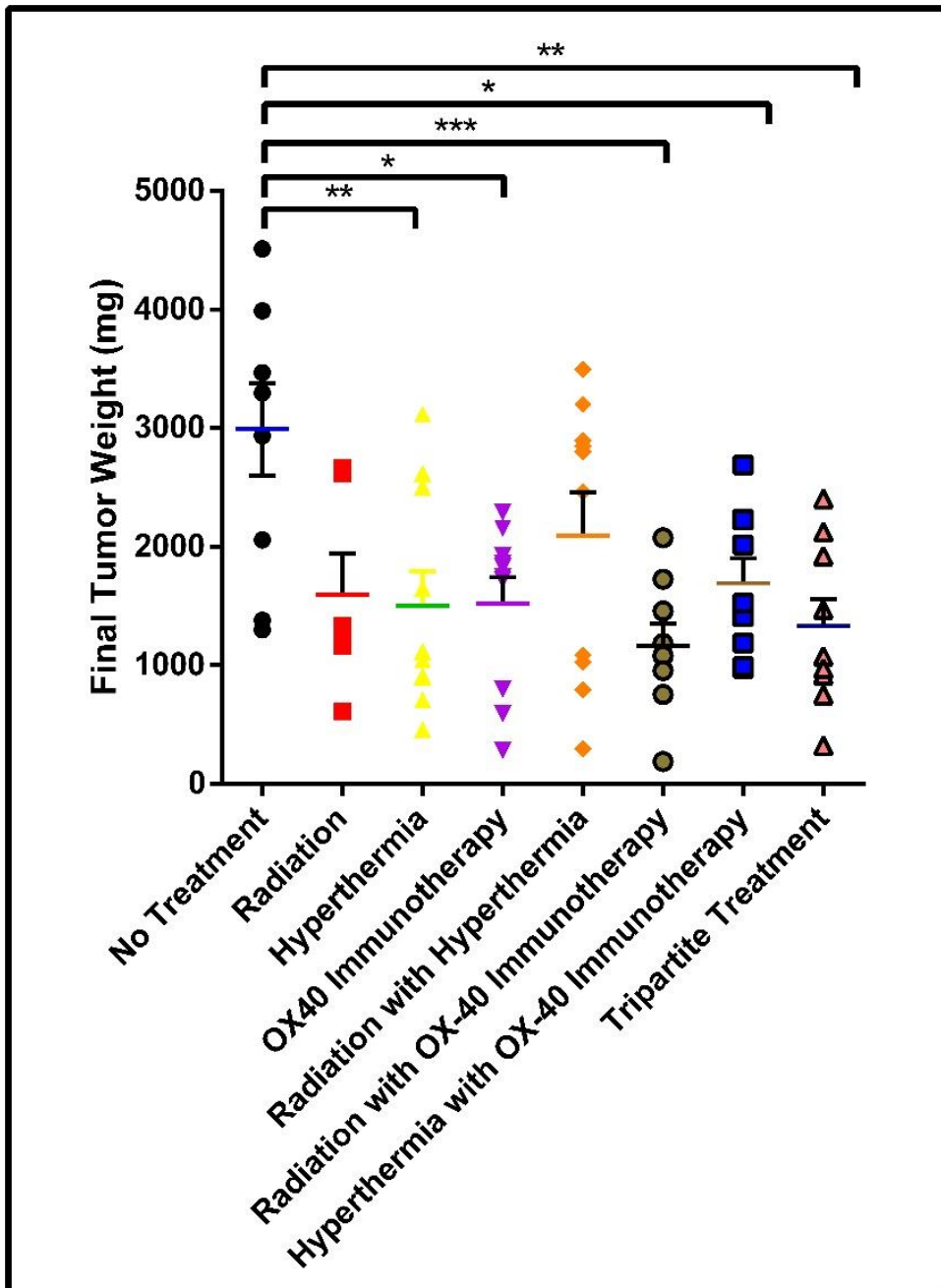
This study was a preliminary analysis exploring the potential of combining radiation, hyperthermia, and immunotherapy to treat pancreatic cancer. In the future arm of this study, we intend to perform histopathological and western blot analysis to better understand the underlying mechanism of each treatment on the outcome contributing toward its overall anti-tumor activity. Also the current standard of care is the chemotherapeutic agent Gemcitabine, which is immune suppressive under normal circumstances. We intend to explore the potential of the tripartite treatment in this study as a neoadjuvant for chemo-sensitization of the pancreatic tumor and as an immune-stimulator when administered post gemcitabine administration.

This study employed the use of Panc02 a mouse origin pancreatic adenocarcinoma cell line. This cell line was used because we needed an immunocompetent mouse to evaluate the effect of immune system and immunotherapy on tumor growth delay. The use of Panc02 was not ideal because unlike stroma rich pancreatic cancer in humans, Panc02 tumors are significantly stroma deficient. In future experiments, we should

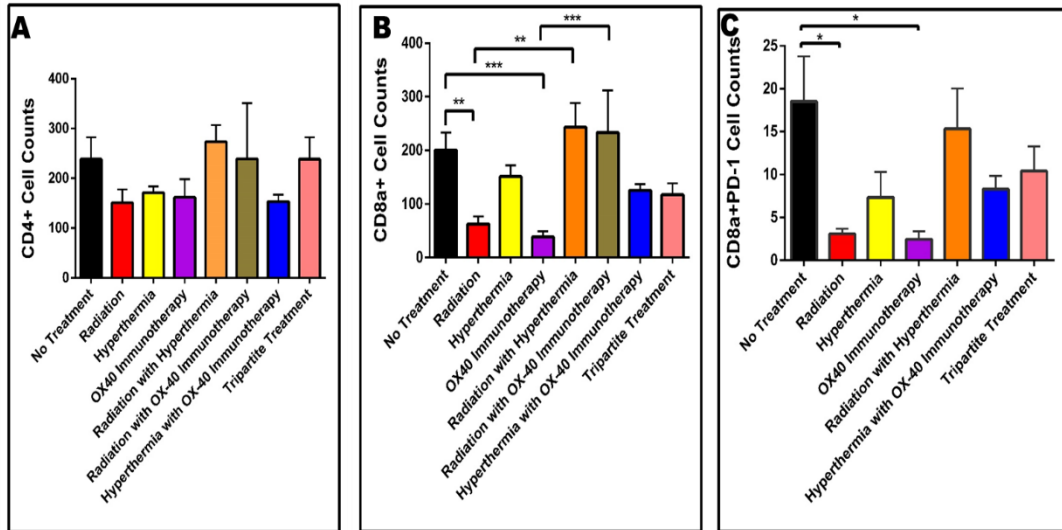
consider the use of animals that develop stroma rich pancreatic tumors. The use of the orthotopic model for pancreatic cancer instead of a subcutaneous model is also an extremely desirable and viable option to explore the development of tumor in three dimensions instead of the current two-dimensional volume estimation.

Furthermore, during flow cytometric analysis neither CD45 nor any live cell markers were utilized. This may be a major drawback that significantly impacts the quality of the flow cytometric analysis. Also, the lack of conclusive flow cytometric outcome could be attributed to the inexperience and lack of in-depth immunological knowledge. In later studies, a detailed immunological analysis should be performed to understand better the pathways contributing towards the anti-tumor effect of this treatment. Therefore in depth analysis will be conducted to explore in detail the distribution of each marker population and the potential consequences of each.

8. Supplementary Figure



Supplementary Figure 1: Aligned dot plot demonstrating the difference in tumor weight between the all different treatment groups (n=10), 'n' demonstrates number of animals per group (mean \pm SEM). *p<0.05, **p<0.01, ***p<0.001



Supplementary Figure 2: (A) Histogram depicting the cell count of CD4+ cells among the total number of lymphocytes in the tumor of animals euthanized 10 days after randomization into study groups; (B) Histogram depicting the cell count of CD8a+ cells among the total number of lymphocytes in the tumor of animals euthanized 10 days after randomization into study groups (mean \pm SEM); (C) Histogram depicting the cell count of CD8a+PD-1+ cells among the total number of lymphocytes in the tumor of animals euthanized 45 days after randomization into study groups (mean \pm SEM) * p <0.05, ** p <0.01, *** p <0.001.

9. References

Ahmadzadeh, M., Johnson, L. a, Heemskerk, B., Wunderlich, J. R., Dudley, M. E., White, D. E., Rosenberg, S. a and Dc, W. (2009) ‘Tumor antigen – specific CD8 T cells infiltrating the tumor express high levels of PD-1 and are functionally impaired Tumor antigen – specific CD8 T cells infiltrating the tumor express high levels of PD-1 and are functionally impaired’, *Blood*, 114(8), pp. 1537–1544. doi: 10.1182/blood-2008-12-195792.

Chatterjee, D. K., Diagaradjane, P. and Krishnan, S. (2011) ‘Nanoparticle-mediated hyperthermia in cancer therapy’, *Therapeutic Delivery*. Future Science Ltd London, UK, 2(8), pp. 1001–1014. doi: 10.4155/tde.11.72.

Chuong, M. D., Springett, G. M., Freilich, J. M., Park, C. K., Weber, J. M., Mellon, E. A., Hodul, P. J., Malafa, M. P., Meredith, K. L., Hoffe, S. E. and Shridhar, R. (2013) ‘Stereotactic body radiation therapy for locally advanced and borderline resectable pancreatic cancer is effective and well tolerated’, *International Journal of Radiation Oncology Biology Physics*. Elsevier Inc., 86(3), pp. 516–522. doi: 10.1016/j.ijrobp.2013.02.022.

Coussens, L. M., Zitvogel, L. and Palucka, A. K. (2013) ‘Neutralizing tumor-promoting chronic inflammation: a magic bullet?’, *Science (New York, N.Y.)*, 339(6117), pp. 286–91. doi: 10.1126/science.1232227.

Curti, B. D., Kovacsovics-Bankowski, M., Morris, N., Walker, E., Chisholm, L., Floyd, K., Walker, J., Gonzalez, I., Meeuwsen, T., Fox, B. A., Moudgil, T., Miller, W., Haley, D., Coffey, T., Fisher, B., Delanty-Miller, L., Rymarchyk, N., Kelly, T., Crocenzi, T., Bernstein, E., Sanborn, R., Urba, W. J. and Weinberg, A. D. (2013) ‘OX40 is a potent immune-stimulating target in late-stage cancer patients’, *Cancer*

Research, 73(24), pp. 7189–7198. doi: 10.1158/0008-5472.CAN-12-4174.

Demaria, S., Bhardwaj, N., McBride, W. H. and Formenti, S. C. (2005) ‘Combining radiotherapy and immunotherapy: A revived partnership’, *International Journal of Radiation Oncology Biology Physics*, 63(3), pp. 655–666. doi: 10.1016/j.ijrobp.2005.06.032.

Demaria, S., Ng, B., Devitt, M. L., Babb, J. S., Kawashima, N., Liebes, L. and Formenti, S. C. (2004) ‘Ionizing radiation inhibition of distant untreated tumors (abscopal effect) is immune mediated’, *International Journal of Radiation Oncology Biology Physics*, 58(3), pp. 862–870. doi: 10.1016/j.ijrobp.2003.09.012.

Feig, C., Gopinathan, A., Neesse, A., Chan, D. S., Cook, N. and Tuveson, D. A. (2012) ‘The pancreas cancer microenvironment’, *Clinical Cancer Research*, 18(16), pp. 4266–4276. doi: 10.1158/1078-0432.CCR-11-3114.

Field, A.-C., Caccavelli, L., Bloch, M.-F. and Bellon, B. (2003) ‘Regulatory CD8+ T cells control neonatal tolerance to a Th2-mediated autoimmunity.’, *Journal of immunology (Baltimore, Md. : 1950)*, 170, pp. 2508–2515. doi: 10.4049/jimmunol.170.5.2508.

Formenti, S. C. and Demaria, S. (2013) ‘Combining radiotherapy and cancer immunotherapy: A paradigm shift’, *Journal of the National Cancer Institute*, 105(4), pp. 256–265. doi: 10.1093/jnci/djs629.

Fresno Vara, J. A., Casado, E., de Castro, J., Cejas, P., Belda-Iniesta, C. and Gonzalez-Baron, M. (2004) ‘PI3K/Akt signalling pathway and cancer’, *Cancer Treat Rev*, 30(2), pp. 193–204. doi: 10.1016/j.ctrv.2003.07.007.

Froger, B. (2003) ‘Danger signals’, *GEO: connexion*, 2(2), pp. 48–49. doi:

10.1038/nm1622.

Garrido-Laguna, I. and Hidalgo, M. (2015) 'Pancreatic cancer: from state-of-the-art treatments to promising novel therapies', *Nature Reviews. Clinical Oncology*. Nature Publishing Group, 12(6), pp. 319–334. doi: 10.1038/nrclinonc.2015.53.

Gough, M. J., Crittenden, M. R., Sarff, M., Pang, P., Seung, S. K., Vetto, J. T., Hu, H.-M., Redmond, W. L., Holland, J. and Weinberg, A. D. (2010) 'Adjuvant therapy with agonistic antibodies to CD134 (OX40) increases local control after surgical or radiation therapy of cancer in mice.', *Journal of immunotherapy (Hagerstown, Md. : 1997)*, 33(8), pp. 798–809. doi: 10.1097/CJI.0b013e3181ee7095.

Gu, P., Fang Gao, J., D'Souza, C. a, Kowalczyk, A., Chou, K.-Y. and Zhang, L. (2012) 'Trogocytosis of CD80 and CD86 by induced regulatory T cells', *Cellular and Molecular Immunology*. Nature Publishing Group, 9(2), pp. 136–146. doi: 10.1038/cmi.2011.62.

Guidelines, C. P. (2005) 'Pancreatic Adenocarcinoma', *Cancer*, pp. 1039–1049. doi: 10.1056/NEJMra1404198.

Hein, A. L., Ouellete, M. M. and Yan, Y. (2014) 'Radiation-induced signaling pathways that promote cancer cell survival (Review)', *International Journal of Oncology*, 45(5), pp. 1813–1819. doi: 10.3892/ijo.2014.2614.

Hirschhorn-Cymerman, D., Rizzuto, G. a, Merghoub, T., Cohen, A. D., Avogadri, F., Lesokhin, A. M., Weinberg, A. D., Wolchok, J. D. and Houghton, A. N. (2009) 'OX40 engagement and chemotherapy combination provides potent antitumor immunity with concomitant regulatory T cell apoptosis.', *The Journal of experimental medicine*, 206(5), pp. 1103–16. doi: 10.1084/jem.20082205.

- Ikemoto, T., Yamaguchi, T., Morine, Y., Imura, S., Soejima, Y., Fujii, M., Maekawa, Y., Yasutomo, K. and Shimada, M. (2006) 'Clinical roles of increased populations of Foxp3+CD4+ T cells in peripheral blood from advanced pancreatic cancer patients.', *Pancreas*, 33(4), pp. 386–90. doi: 10.1097/01.mpa.0000240275.68279.13.
- Klemm, F. and Joyce, J. A. (2015) 'Microenvironmental regulation of therapeutic response in cancer', *Trends in Cell Biology*. Elsevier Ltd, 25(4), pp. 198–213. doi: 10.1016/j.tcb.2014.11.006.
- Laheru, D. and Jaffee, E. M. (2005) 'Immunotherapy for pancreatic cancer - science driving clinical progress.', *Nature reviews. Cancer*, 5(6), pp. 459–467. doi: 10.1038/nrc1630.
- Leigue, L. and Moore, B. A. (2016) 'Antimicrobial susceptibility and minimal inhibitory concentration of *Pseudomonas aeruginosa* isolated from septic ocular surface disease in different animal species', 6, pp. 215–222. doi: 10.4314/ovj.v6i3.9.
- Li, D. H., Xie, K. P., Wolff, R. and Abbruzzese, J. L. (2004) 'Pancreatic cancer', *Lancet*, 363, pp. 1049–1057. doi: Doi 10.1016/S0140-6736(04)15841-8.
- Ma, W. W. and Hidalgo, M. (2013) 'The winning formulation: The development of paclitaxel in pancreatic cancer', *Clinical Cancer Research*, 19(20), pp. 5572–5579. doi: 10.1158/1078-0432.CCR-13-1356.
- Malyutina, Y. V., Makarova, Y. M., Semenets, T. N., Semina, O. V., Mosin, A. F. and Kabakov, A. E. (2005) 'Whole body hyperthermia in mice confers heat shock protein-dependent radioresistance of their bone marrow and thymocytes', *Journal of Thermal Biology*, 30(7), pp. 511–517. doi: 10.1016/j.jtherbio.2005.06.003.
- Melrose, J., Perroy, R., Careas, S., Martin, L. P., Hamilton, T. C., Schilder, R. J.,

- Helleday, T., Petermann, E., Lundin, C., Hodgson, B. and Sharma, R. A. (2008) 'DNA repair pathways as targets for cancer therapy', *Nat Rev Cancer*, 14(3), pp. 1291–1295. doi: 10.1017/CBO9781107415324.004.
- Moncharmont, C., Levy, A., Guy, J. B., Falk, A. T., Guilbert, M., Trone, J. C., Alphonse, G., Gilormini, M., Ardail, D., Toillon, R. A., Rodriguez-Lafrasse, C. and Magn??, N. (2014) 'Radiation-enhanced cell migration/invasion process: A review', *Critical Reviews in Oncology/Hematology*. Elsevier Ireland Ltd, 92(2), pp. 133–142. doi: 10.1016/j.critrevonc.2014.05.006.
- De Monte, L., Reni, M., Tassi, E., Clavenna, D., Papa, I., Recalde, H., Braga, M., Di Carlo, V., Doglioni, C. and Protti, M. P. (2011) 'Intratumor T helper type 2 cell infiltrate correlates with cancer-associated fibroblast thymic stromal lymphopoietin production and reduced survival in pancreatic cancer.', *The Journal of experimental medicine*, 208(3), pp. 469–78. doi: 10.1084/jem.20101876.
- Moran, A. E., Kovacsovics-Bankowski, M. and Weinberg, A. D. (2013) 'The TNFRs OX40, 4-1BB, and CD40 as targets for cancer immunotherapy', *Current Opinion in Immunology*. Elsevier Ltd, 25(2), pp. 230–237. doi: 10.1016/j.coi.2013.01.004.
- Morgan, M. a. and Lawrence, T. S. (2015) 'Molecular Pathways: Overcoming Radiation Resistance by Targeting DNA Damage Response Pathways', *Clinical Cancer Research*, 21(13), pp. 2898–2904. doi: 10.1158/1078-0432.CCR-13-3229.
- Nascimbeni, M., Shin, E. C., Chiriboga, L., Kleiner, D. E. and Rehermann, B. (2004) 'Peripheral CD4+CD8+ T cells are differentiated effector memory cells with antiviral functions', *Blood*, 104(2), pp. 478–486. doi: 10.1182/blood-2003-12-4395.
- Nomi, T., Sho, M., Akahori, T., Hamada, K., Kubo, A., Kanehiro, H., Nakamura, S., Enomoto, K., Yagita, H., Azuma, M. and Nakajima, Y. (2007) 'Clinical significance

and therapeutic potential of the programmed death-1 ligand/programmed death-1 pathway in human pancreatic cancer', *Clinical Cancer Research*, 13(7), pp. 2151–2157. doi: 10.1158/1078-0432.CCR-06-2746.

Ohuchida, K., Mizumoto, K., Murakami, M., Qian, L., Sato, N., Nagai, E., Matsumoto, K., Nakamura, T. and Tanaka, M. (2004) 'Radiation to Stromal Fibroblasts Increases Invasiveness of Pancreatic Cancer Cells through Tumor-Stromal Interactions Radiation to Stromal Fibroblasts Increases Invasiveness of Pancreatic Cancer Cells through Tumor-Stromal Interactions 1', pp. 3215–3222. doi: 10.1158/0008-5472.CAN-03-2464.

Parel, Y. and Chizzolini, C. (2004) 'CD4+ CD8+ double positive (DP) T cells in health and disease', *Autoimmunity Reviews*, 3(3), pp. 215–220. doi: 10.1016/j.autrev.2003.09.001.

Patrick Michl, T. M. G. (2013) 'Current concepts and novel targets in advanced pancreatic cancer', *Gut*, 62(800), pp. 317–326. doi: 10.1136/gutjnl-2012-303588.

Postow, M. A., Callahan, M. K. and Wolchok, J. D. (2015) 'Immune Checkpoint Blockade in Cancer Therapy.', *Journal of clinical oncology : official journal of the American Society of Clinical Oncology*, 33(17), p. JCO.2014.59.4358-. doi: 10.1200/JCO.2014.59.4358.

Rotstein, S., Blomgren, H., Petrini, B., Wasserman, J. and Baral, E. (1985) 'Long term effects on the immune system following local radiation therapy for breast cancer. I. Cellular composition of the peripheral blood lymphocyte population.', *International journal of radiation oncology, biology, physics*, 11(5), pp. 921–925. doi: 10.1016/0360-3016(85)90114-2.

Safe, S. (2015) 'Targeting apoptosis pathways in cancer - Letter', *Cancer Prevention*

Research, 8(4), p. 338. doi: 10.1158/1940-6207.CAPR-14-0405.

Sideras, K., Braat, H., Kwekkeboom, J., van Eijck, C. H., Peppelenbosch, M. P., Sleijfer, S. and Bruno, M. (2014) 'Role of the immune system in pancreatic cancer progression and immune modulating treatment strategies', *Cancer Treatment Reviews*. Elsevier Ltd, 40(4), pp. 513–522. doi: 10.1016/j.ctrv.2013.11.005.

Siegel, R., Miller, K. and Jemal, A. (2017) 'Cancer statistics , 2017 .', *CA Cancer J Clin*, 67(1), pp. 7–30. doi: 10.3322/caac.21254.

Singh, D., Upadhyay, G., Srivastava, R. K. and Shankar, S. (2015) 'Recent advances in pancreatic cancer: biology, treatment, and prevention.', *Biochimica et biophysica acta*. Elsevier B.V., 1856(1), pp. 13–27. doi: 10.1016/j.bbcan.2015.04.003.

Soares, P. I., Ferreira, I. M., Igreja, R. A., Novo, C. M. and Borges, J. P. (2012) 'Application of hyperthermia for cancer treatment: recent patents review', *Recent Pat Anticancer Drug Discov*, 7(1), pp. 64–73. Available at: <http://www.ncbi.nlm.nih.gov/pubmed/21854362>.

Stathis, A. and Moore, M. J. (2010) 'Advanced pancreatic carcinoma: current treatment and future challenges.', *Nature reviews. Clinical oncology*. Nature Publishing Group, 7(3), pp. 163–172. doi: 10.1038/nrclinonc.2009.236.

Teng, L. S., Jin, K. T., Han, N. and Cao, J. (2010) 'Radiofrequency ablation, heat shock protein 70 and potential anti-tumor immunity in hepatic and pancreatic cancers: A minireview', *Hepatobiliary and Pancreatic Diseases International*, 9(4), pp. 361–365.

Valsecchi, M. E., Díaz-Cantón, E., De La Vega, M. and Littman, S. J. (2014) 'Recent treatment advances and novel therapies in pancreas cancer: A review', *Journal of*

Gastrointestinal Cancer, 45(2), pp. 190–201. doi: 10.1007/s12029-013-9561-z.

Vasievich, E. A. and Huang, L. (2011) ‘The suppressive tumor microenvironment: A challenge in cancer immunotherapy’, *Molecular Pharmaceutics*, 8(3), pp. 635–641. doi: 10.1021/mp1004228.

Vazquez, A., Bond, E. E., Levine, A. J. and Bond, G. L. (2008) ‘The genetics of the p53 pathway, apoptosis and cancer therapy.’, *Nature reviews. Drug discovery*, 7(12), pp. 979–87. doi: 10.1038/nrd2656.

Victor, C. T.-S., Rech, A. J., Maity, A., Rengan, R., Pauken, K. E., Stelekati, E., Benci, J. L., Xu, B., Dada, H., Odorizzi, P. M., Herati, R. S., Mansfield, K. D., Patsch, D., Amaravadi, R. K., Schuchter, L. M., Ishwaran, H., Mick, R., Pryma, D. A., Xu, X., Feldman, M. D., Gangadhar, T. C., Hahn, S. M., Wherry, E. J., Vonderheide, R. H. and Minn, A. J. (2015) ‘Radiation and dual checkpoint blockade activate non-redundant immune mechanisms in cancer’, *Nature*, 520(7547), pp. 373–377. doi: 10.1038/nature14292.

Vincent, A., Herman, J., Schulick, R., Hruban, R. H. and Goggins, M. (2011) ‘Pancreatic cancer’, *The Lancet*. Elsevier Ltd, 378(9791), pp. 607–620. doi: 10.1016/S0140-6736(10)62307-0.

Zheng, L., Jr, L. A. D., Donehower, R. C. and Jaffee, E. M. (2014) ‘Previously Treated Pancreatic Cancer’, 36(7), pp. 382–389. doi: 10.1097/CJI.0b013e31829fb7a2.Evaluation.

Key Statistics for Pancreatic Cancer, <https://www.cancer.org/cancer/pancreatic-cancer/about/key-statistics.html> (accessed May 09, 2017). Key Statistics for Pancreatic Cancer, <https://www.cancer.org/cancer/pancreatic-cancer/about/key-statistics.html> (accessed May 09, 2017).